Application of Texture Analysis to Functional Pulmonary CT Data

Meier, Arndt; Farrow, Catherine; Harris, Benjamin; King, Gregory; Jones, Alan

Published in:
Computerized Medical Imaging and Graphics

DOI:
10.1016/j.compmedimag.2011.01.001

2011

Elsevier Editorial System(tm) for Computerized Medical Imaging and Graphics
Manuscript Draft

Manuscript Number:

Title: Application of Texture Analysis to Functional Pulmonary CT Data

Article Type: Full Length Article

Section/Category:

Keywords: texture analysis, computed tomography, asthma, COPD, lung ventilation

Corresponding Author: Dr Arndt Meier,

Corresponding Author's Institution: University of Sydney

First Author: Arndt Meier

Order of Authors: Arndt Meier; Catherine Walsh; Benjamin E Harris; Gregory G King; Allan Jones, Dr

Manuscript Region of Origin:

Abstract: Abstract
It is demonstrated that textural parameters calculated from functional pulmonary CT data have the potential to provide a robust and objective quantitative characterisation of inhomogeneity in lung function and classification of lung diseases in routine clinical applications. Clear recommendations are made for optimum data preparation and textural parameter selection.
A new set of platform-independent software tools are presented that are implemented as plug-ins for ImageJ. The tools allow segmentation and subsequent histogram-based and grey-level co-occurrence matrix based analysis of the regions of interest. The work-flow is optimised for use in a clinical environment for the analysis of transverse Computed Tomography (CT) scans and lung

ventilation scans based on SPECT. Consistency tests are made against other texture analysis plug-ins and simulated lung CT data. The same methods are then applied to patient data consisting of a healthy reference group and one patient group each who suffered from asthma, chronic obstructive pulmonary disease (COPD), and COPD plus lung cancer. The potential for disease classification based on computer analysis is evaluated.

Application of Texture Analysis to Functional Pulmonary CT Data

Arndt Meier[a], Catherine Walsh[b,c,d], Benjamin E. Harris[b,c,d], Gregory G.King[b,c,d], and Allan Jones[a]

a) Australian Key Centre for Microscopy and Microanalysis, The University of Sydney, Sydney 2006, NSW, Australia, email: a.meier@usyd.edu.au *(corresponding author)*

b) Department of Respiratory Medicine, Royal North Shore Hospital, St Leonards NSW 2065

c) Woolcock Inst. of Medical Research, 431 Glebe Point Road, Glebe, NSW 2037

d) Northern Clinical School, Faculty of Medicine, University of Sydney, Sydney, 2006

Abstract

It is demonstrated that textural parameters calculated from functional pulmonary CT data have the potential to provide a robust and objective quantitative characterisation of inhomogeneity in lung function and classification of lung diseases in routine clinical applications. Clear recommendations are made for optimum data preparation and textural parameter selection.

A new set of platform-independent software tools are presented that are implemented as plug-ins for ImageJ. The tools allow segmentation and subsequent histogram-based and grey-level co-occurrence matrix based analysis of the regions of interest. The work-flow is optimised for use in a clinical environment for the analysis of transverse Computed Tomography (CT) scans and lung ventilation scans based on SPECT. Consistency tests are made against other texture analysis plug-ins and simulated lung CT data. The same methods are then applied to patient data consisting of a healthy reference group and one patient group each who suffered from asthma, chronic obstructive pulmonary disease (COPD), and COPD plus lung cancer. The potential for disease classification based on computer analysis is evaluated.

KEYWORDS:

texture analysis, computed tomography, asthma, COPD, lung ventilation

1. Introduction

Close to 10 percent of the world population are suffering from chronic lung diseases. The two most common categories, which account for 7.7%, are asthma and chronic obstructive pulmonary disease (COPD).

According to World Health Organisation (WHO) estimates, 300 million people suffer from asthma and 255 000 people died of asthma in 2005 (WHO, 2008a) and an increase of 20% is expected over the next 10 years. Asthma is the most common chronic disease among children. It is characteried by episodic airway narrowing that occurs on exposure to stimuli, such as exercise, dust, pollens and cold air. Asthmatic lungs are characterised by inhomogeneous ventilation when studied by pulmonary function techniques or by imaging methods. The severity of the inhomogeneity, measured by pulmonary function, is strongly related to the sensitivity of airways to inhalants, i.e. dust, pollens etc. Thus characterisation of the topographical pattern of ventilation in asthmatic lungs is important

The WHO estimates (2007), currently 210 million people suffer from chronic obstructive pulmonary disease (COPD) with 3 million people dying of COPD in 2005 (WHO, 2008b). COPD is a chronic disease that is caused predominantly by tobacco smoking in western countries. COPD causes lung destruction, known as emphysema, and diseases of small and large airways, which result in cough, mucous production and airway narrowing with resultant breathlessness during exertion.

Single-photon emission computed tomography (SPECT) ventilation scanning (Petersson *et al.*, 2007) using Technetium-99 (Technegas™), is a three dimensional imaging technique used routinely in clinical nuclear medicine for diagnosis of diseases such as pulmonary embolism, when combined with imaging of blood flow (Harris *et al.*, 2007). Ventilation scans, however, have been adapted for studies of ventilation in airways disease (King *et al.,* 1997 and 1998,

Downie *et al.*, 2007). SPECT imaging offers the potential to characterise the topographical distribution of ventilation so that inhomogeneity can be quantified at the regional level (Xu *et al.*, 2001, Venegas *et al.*, 2005). Combining imaging information with the pulmonary function measures of inhomogeneity will provide important information about the ventilatory abnormalities in asthma and COPD (Tgavalekos *et al.,* 2007, Berend *et al.*, 2008). However, suitable methods for quantifying the distribution of ventilation from SPECT data have not been determined.

In this study, we investigate several potentially useful methods of quantifying the distribution of ventilation from SPECT ventilation data using both simulated SPECT data and data from well-described clinical groups. The new technique is based on texture analysis and can provide an objective indicator of abnormal lung conditions.

2. Methods

We developed new techniques for multiple 3D texture analysis and conventional 3D image analysis of clinical SPECT data of volumes representing lung tissue as identified from co-registered CT scans that were obtained at the time of the SPECT.

The new technique uses the anatomical CT to define the lung outlines, co-registers these with the functional SPECT data and performs an image analysis on the voxels of the SPECT thus defined as representing lung tissue. The image analysis comprises a traditional direct analysis of the grey levels in the SPECT slices and a texture parameters analysis derived from grey-level co-occurrence matrices (GLCM) (Haralick, *et al.*, 1973, Choi, 2006).

2.1 Simulation data

We created a series of SPECT-V data sets based on simulated data to validate the software. The lung phantom used in the construction of the model was based upon X-ray computed tomography (CT) data from a male of height 178 cm, weighing 70 kg (Zubal *et al.*, 1994) in supine position, who was chosen for his similarity to the dosimetry standard mathematical phantom. The Monte Carlo simulation package used for this work was the Photon History Generator (Lewellen *et al.*, 1988, Haynor *et al.*,1991), which models the emission, scatter and attenuation of photons in a heterogeneous phantom, followed by the photons' subsequent collimation and detection (Chicco *et al.*, 2001).

Simulations were performed for a 23.6-mm-thick parallel-hole collimator, using a 32.5-cm radius of rotation. The isotope modelled was Tc99, collected with a symmetric 20% energy window centred around 140 keV into a 128×128 matrix with 120 views at equal angular spacing around 360°, resulting in 5 million counts total when no defects were present. Pixel resolution was 2.5mm/pixel. To test for any dependence on brightness changes we repeated two simulations with 9 million counts. These settings were chosen to closely mimic typical clinical settings when collecting SPECT-V data (similar contrast, spatial resolution and signal to noise).

A series of studies were performed in four groups, distinguished by the size of individual defects, to simulate the effects of non-ventilated lung tissue. Defects in groups 1–4 were 1x1x1 pixels (15 mm^3), 2x2x2 pixels (125 mm^3), 3x3x3 pixels (422 mm^3) and 4x4x4 pixels (1000 mm^3) in size, respectively. These were distributed uniformly throughout both lung halves in a random manner. Within each group, the amount of lung tissue involved in defects varied from 0% (normal) up to 40% in steps of 5%, giving 9 studies in each group.

These simulated lung data sets were then subjected to normal clinical processing. Lungs were reconstructed at the same resolution as routine SPECT data (128 slices with 128x128 pixels, voxel size 4.664mm^3). The lung outlines were known from the original phantom and

converted to a binary mask which was then subjected to 2 iterations with the standard ImageJ erosion operation using a count of 3 (minimum 3 of the nearest neighbour pixels need to be background pixels for the present pixel to be eroded).

2.2 Clinical data

Three groups of patients were studied to evaluate the applicability of the new methods. Five patients had asthma (data set A), and 10 current or ex-smokers that had either diagnosed COPD (data set C) or were being evaluated for treatment of lung cancer (PELICAN[1] data set) who had a wide range of severity of COPD, and scans from 5 patients who underwent lung scanning for suspected pulmonary embolism but who were considered to have normal lung scans on routine clinical assessment (data set N).

All subjects inhaled Technegas as the ventilation imaging agent. Patients had scans according to the standard clinical protocol whereby Technegas was inhaled from the Technegas generator by 1-2 deep inspirations followed by a breath hold to maximise Technegas particle deposition.

Subjects had a ventilation SPECT scan and a CT scan acquired by a dual-detector variable angle hybrid SPECT/CT system (Phillips SKYLight and Picker PQ5000 CT). All SPECT studies were acquired using a 128 x 128 matrix, at 15 seconds per stop with 3 degree steps over 360 degrees. Low-dose CT was performed using non-contrast (30mA, 10kVp, pitch 1.5, slice thickness 4mm). Study was acquired during tidal breathing. CT images are reconstructed using a 512 x 512 matrix with a smooth algorithm.

Spirometry, including the predicted forced experitory volume during one second (FeV1), was obtained in all groups except the normal group, using standard methods in the lung function

[1]PELICAN study: Predicting Exercise tolerance and Lung function using Imaging in patients undergoing CANcer Surgery, Royal North Shore Hospital, internal study, 2007.

laboratory.

2.3 Software

Custom plug-ins were developed for ImageJ (Rasband, 1997-2008) to read and write CT data routinely stored in Interfile data format (Cradduck et al., 1989). Segmentation of the lungs in the CT datasets is done with a custom written plug-in "Extract_Lungs", which was more efficient than existing segmentation plug-ins (Parker, 2008, Castleman, 2005). Segmentation uses an edge-following algorithm that stays between an upper and lower grey-value threshold. If the initial seed-point falls outside the thresholds, a new seed-point is automatically determined from a search towards the median point of the previous slice and an outward spiral from there if that fails.

Up to 5 regions of interest per slice are supported which are categorised as belonging to either the left or right lungs. A custom-built ROI manager allows superimposition of the ROIs onto SPECT ventilation data. The identified volumes are analysed for total area, mean, median, modal, minimum, and maximum grey values, kurtosis, integrated optical density (IOD), and histogram. Weighted means are calculated for left, right and total lung.

Anatomical CT data were registered to corresponding functional data (SPECT) with the ImageJ plug-in Align3_TP (Parker, 2008) with all parameters left to their default values. The outlines of the registered lung mask were then auto-detected with our segmentation algorithm resulting in ImageJ standard ROIs (regions of interest). Our modified ROI manager limits all subsequent analysis to within the defined ROIs.

From these ROIs that represent the total lung volume, GLCMs are calculated for the x, y, z, and invariant orientation for a set of up to 5 chosen distances. These are then subjected to standard texture analysis. We verified the correct implementation of the GLCM algorithm by

comparing results from an independently written plug-in [Cabrera, 2005], which calculates 4 of the 12 textural features we determine, and found both to be consistent.

Our methods are based on software that is easily available, widely used, modular in design, open source and not limited to a specific operating system. ImageJ (Rasband, 1997-2008), Abramoff *et al.*, 2004, Burger & Burge, 2008) fulfils all these criteria perfectly. And more so, there is a very large collection of plug-ins publicly available (http://rsb.info.nih.gov/ij/plugins/). The code used in this study is available from the author.

2.4 Analysis

In both the simulated and the clinical data the volumes representing lung tissue were identified as described above. All voxels outside the eroded ROIs were excluded from the analysis. Note that lung tissue outlines were registered to the reconstructed SPECT data, thus avoiding any interpolation in the SPECT data set.

All SPECT data sets, simulated and clinical, were prepared in two parallel streams: *CS* (contrast stretched) and *HM* (histogram matched). The contrast stretched data set was created by first stretching the contrast within the 16-bit grey-levels image stack using the stack histogram (built-in ImageJ function) and then converting the image stack to an 8-bit grey-level image stack. The latter step used an improved version of the ImageJ Stack Converter that uses the stack histogram as opposed to the histogram of the current slice and allows to fold a set percentage of hot pixels into the highest remaining histogram channel. We chose the 0.02% brightest non-background pixels to be treated as hot pixels.

The histogram-matched data set used the histogram from the best ventilated simulated lung as the reference histogram after smoothing it twice with a Gaussian filter of 5 histogram channels width. This histogram compared well with histograms obtained from patients with

normal lung function. The histogram matcher we wrote uses the stack histogram and can directly map a 16-bit image stack onto an 8-bit reference histogram thus considerably reducing channel pile-up effects commonly encountered when first converting from 16-bit to 8-bit and then again from 8-bit to 8-bit reference histogram.

The 'extracted lungs' as defined by sets of ROIs were then analysed in two steps. The normal grey value analysis calculated the total lung volume in voxels, the ventilated volume, the minimum, mean, modal, median and maximum grey values, IOD, contrast, histogram, and Kurtosis on a per-ROI basis. Mean values weighted by ROI area were calculated for left, right, and total lung.

A voxel was considered to represent ventilated lung tissue if it had a grey value larger than 20% of the histogram maximum. To minimise the impact of any erratic hot pixels, the histogram maximum was calculated from the 97% level assuming that the histogram above 97% drops with a slope of -0.5. In this work we only report the results for total lungs, but it is noted that the software reports more details where this may be of interest.

The second step of the analysis created 8-bit grey-level co-occurrence matrices (GLCMs) from all the ROIs of any one lung for 5 distances each: 1, 2, 4, 8, and 12 pixels (4.7, 9.3, 18.7, 37.3, 56.0mm) and for 4 direction pairs each: X (left->right, right->left), Y (top->bottom, bottom->top), Z (up->down, down->up) and I (invariant, combining X, Y, and Z). The invariant matrix we chose gives equal weight to each valid voxel pair and may at times differ from a mean over the X, Y, and Z matrices as individual matrices may not have the exact same number of voxel pairs. From these GLCMs twelve texture features were calculated as listed in appendix A (Haralick *et al.*, 1973, Haralick 1979, Choi, 1996).

3. Results

3.1 Results from the phantom study

The texture parameters calculated from the simulated lungs show a number of correlations with the size of the defects and the total non-ventilated volume (NVV). Figure 1 illustrates this for the example of the textural parameter TC18 (coefficient of variation) and simulated defect sizes of 3x3x3 pixels. For all GLCM distances and defect sizes the parameter TC18 increases steadily with increasing NVV and more rapidly so for larger defects.

No significant differences were found between results obtained from X, Y, and Z GLCMs. Hence only the invariant GLCMs have been studied further. For all 12 textural parameters studied we found under all conditions that the functions such as in Figure 1 are smooth and steady and that different distances in GLCM calculation result in slightly shifted versions of the same shape but that in no case does the graph of one distance cross the graph of another distance for otherwise identical settings. On the contrary, we often saw that graphs for different distances were almost undistinguishable from one another. Consequently the data from all distances were pooled into one; thus reducing the complexity of the results presented. Notwithstanding this, it is noted, that TC9 and TC30 were somewhat more sensitive to NVV changes at shorter distances and that TC2 showed no dependence on NVV but gave significantly different results for different distances.

For clarity only the relative changes in textural parameters between the lowest and highest NVV studied are reported, because the functions change smoothly with NVV and in-between values do not add much to the discussion.

Table 1 lists the relative changes in the textural parameters calculated in response to a 40% drop in ventilated lung volume. Some textural parameters are more sensitive to the changes in ventilated volume than others as can be seen from Table 1 (rows 6 and 11 "*mean*"). Also, they are typically stronger in the contrast-stretched data set (***cs***, row 6) as compared to the

histogram-matched data set (***hm***, row 11).

The results from a sensitivity test to brightness changes are shown in Table 2. We repeated the simulation for the "worst" lung with a higher activity such that after adding the defects it resulted in the same IOD as the perfectly ventilated simulated lung. Insensitivity to brightness changes would allow the direct comparison of textural parameters derived from studies that use different gamma counts. Note that rows 2 and 3 in Table 2 correspond to rows 5 and 10 in Table 1 (10 mm), respectively, but the percentage changes are expressed relative to the values in Table 1. It is noted that the sign of all values in Table 2 act in such a way as to reduce the sensitivity of the textural parameters.

In the context of our work a good textural parameter is one that is sensitive to changes in NVV or defect-size and that is at the same time insensitive to changes in brightness. With this in mind we can group the textural parameters investigated into robust, intermediate and poor performers:

Robust textural parameters:

TC13/TC31 Variance/Mean ratio: provides a solid signal of 22% change in the parameter value for a 40% change in NVV while its dependence on brightness doubling is only small (1.5%). The sensitivity is somewhat poorer for smaller defects.

TC30 Local homogeneity: provides still a good signal of 10.5% change for a 40% drop in NVV but is more sensitive to brightness changes than the TC13/TC31 ratio (2.9%).

TC18 Coefficient of Variation: provides a very strong signal of 77% for large defects and a still strong signal of 22% for small defects. It has a moderate dependence on brightness changes (10.8% simulating large defects). However, correlation with clinical data discussed below is excellent.

Textural parameters with intermediate performance:

TC1 Angular second moment: provides high sensitivity (>68%) to changes in NVV, but unfortunately it is also very sensitive to brightness changes.

TC2 and TC2: Difference and inverse difference moment: show a modest sensitivity for short distances and small-sized defects but are insensitive at larger pixel distances as well as for larger defect sizes. However, they may be used successfully in conjunction with other parameters to decide whether the effective size distribution of the non-ventilated volumes is small or large.

TC9 Correlation: The theoretical study shows a reasonable sensitivity of around 20% to changes twice that large in NVV but also a relatively high sensitivity to brightness changes. In the clinical studies discussed below this parameter did not convince and is outperformed by others.

Textural parameters with poor performance:

TC7, TC4, TC13, TC31, TC21, and TC23: These parameters suffer either from a lack of sensitivity or high sensitivity to changes in brightness.

Combination of textural parameters:

The ratio of TC13/TC31 is a very good performer although neither TC13 nor TC31 are good performers. Similarly, the ratio of TC21/TC31 gives a moderately good performance.

3.2 Results from the clinical studies

Figure 2 illustrates the estimated ventilated lung volume grouped by patient group. The 'normal' group shows the highest ventilated volume of about 90% and the smallest variance. Asthmatic lungs at baseline show a slightly lower ventilated lung volume although not statistically significant from the 'normal' lungs. The remaining patient groups show significant reductions in ventilated lung volume that are strongest in COPD patients. There is also a higher variability in these groups.

Figures 3 and 4 illustrate one of the best performing textural parameters for the 5 patient groups studied. Both the absolute value and the variability between different GLCM distances and between patients in the 'normal' lung function group are small (Figure 3, left panel). The results from COPD patients which range from a mild case (right panel, c-01) to severe (c-05) show increasingly higher values.

The differences between using different distances in the GLCM calculations are almost within the numerical precision, which was also observed in the results from the simulated data. This observation holds true for all textural parameters and patient groups studied except for TC2, TC9 and TC30. TC9 (Correlation) and TC30 (Local Homogeneity) lose sensitivity with increasing distance between voxel pairs and better performance is achieved by only using the 2 shortest distances (1 and 2 pixels distance corresponding to 4.7 and 9.3mm, respectively). TC2 will be discussed separately below. These findings are consistent with observations from the simulated data.

Pooling the data from all GLCM distances[2] and by patient group allows us to look for disease-specific differences as shown in Figure 4.While asthmatics at baseline cannot be distinguished from normal lungs, they can be clearly identified after a Metacholine challenge. PELICAN patients and even more so COPD patients have strongly elevated values in the coefficient of variation calculated from the GLCM.

[2] Except for TC9 and TC30 which pooled only the 2 shortest distances for higher sensitivity

Figure 5 presents the ratio of Local Homogeneity and GLCM Mean (TC30/TC31) calculated in the same way as in the previous figure. Again, values for COPD and PELICAN patients are significantly higher than those for normal and asthmatic lungs. It is noted, however, that asthma patients both at baseline and at Metacholine challenge give almost identical results. Hence combining the information from multiple textural parameters allows to distinguish between different disease classes such as asthma from COPD.

A very strong correlation (r^2=0.955) between the textural parameter Coefficient of Variation (TC18) and the estimated ventilated lung volume is illustrated in Figure 6. Similarly high correlations of r^2>0.8 exist for textural parameters TC3, TC30, TC31, and the ratios TC13/TC31 and TC21/TC31 as a function of ventilated lung volume (not illustrated). More positive correlations (r^2>0.49) are observed for textural parameters TC1, TC9, and the ratio TC1/TC31.

Independent spirometry data in the form of the predicted forced expiratory volume during 1 second (FeV1) was available for all but the 'normal' group. Again good correlations are observed with several textural parameters (r^2>0.5 for TC18 and TC13/TC31, r^2>0.4 for TC3, TC30, TC21/TC31, TC31 and TC1/TC31 and r^2>0.3 for TC1, TC2 and TC9) as illustrated in Figure 7 for the example of TC13/TC31.

The Difference Moment (TC2) behaves differently from all other textural parameters studied. It is insensitive to changes in both NVV and FeV1, but it is sensitive to the size distribution of patterns in the lung. Hence the TC2 textural parameter results were prepared in a different way. Instead of pooling the results from different GLCM distances, the parameter value obtained with the shortest distance (1 pixel) were divided by the parameter value for the second largest distance for any one lung and that we refer to as $TC2_d$ for short. Data prepared in this way resulted in a positive correlation of $TC2_d$ with NVV (r^2=0.69) and a somewhat weaker correlation with FeV1 (r^2=0.375).

All results in this section were derived from the contrast-stretched data set as it showed an overall better performance than compared to results derived from the histogram-matched data. It is noted that TC18, TC31 (Mean) and TC13/TC31 were indifferent to both NVV and FeV1 changes in the histogram-matched data set, but otherwise the same textural parameters performed well as in the contrast-stretched data set. The only textural parameter that faired significantly better in the histogram-matched data set was TC23 (Difference Entropy).

4 Discussion

Changes in the grey level distribution such as a shift to darker grey values – as can be expected with a reduction in ventilated lung volume – is essentially removed in the histogram-matched data. Hence, changes in the textural parameters that occur in the contrast-stretched data set but not in the histogram-matched one are thought to be driven by histogram changes while changes that occur in the histogram-matched data set are thought to be dominated by changes in pattern (Table 1). Changes in the contrast-stretched data set are often a result of both histogram and pattern changes.

In an ideal system a change in brightness should not affect the textural parameters calculated because the GLCMs are always normalised to an IOD of unity. However, it is noted that the spatial resolution of the observation system is significantly lower than the features that cause them. The effective resolution in the SPECT-V data is lower than the pixel resolution of 4.664mm/pxl which in turn is much coarser than the simulated small defects starting from 2.5mm cube side length. Due to the nature of discrete sampling – and in this case significant under-sampling – of the object space and the non-linearity of the resulting effective blurring, the texture parameters calculated become dependent on the total optical density and contrast in the SPECT-V data sets. This effect itself is also dependent on the effective size distribution

of the defects we seek to describe. To quantitatively describe the exact relationship is mathematically complex and of limited practical use as it will vary from situation to situation. Instead we seek to identify textural parameters that depend acceptably little on the variability in patient data preparation.

The simulated data allows to fully control the environment, to know the true size distribution of the non-ventilated lung volumes, the true ventilated volume, and to vary some of these parameters systematically to study its impact. However, there are also some differences and limitations compared to clinical data that are undesirable. One is that the IOD of the simulated SPECT-V scan drops progressively with increasing NVV due to the simplicity of the model available to us.

A patient with a smaller ventilated lung volume inhales approximately the same amount of radioactivity as a patient with a larger ventilated lung volume. As a result the scan from the former patient would have a larger information content[3] and image contrast; because the same amount of activity has to squeeze into a smaller volume, a wider range of different brightness values is observed. Hence a poorly ventilated *simulated* lung has a somewhat *lower* information content in the simulated data in contrast to a patient with a poorly ventilated lung that would result in a *higher* information content than the ideally ventilated lung. We studied this behaviour by simulating one data set with a higher gamma count, which resulted in an increase of 38% in information content as opposed to a 9% drop in the non-corrected simulation case. Although the textural parameters are modified as a result, it does not change the overall response to NVV and we were able to identify textural parameters that are little or non-susceptible to this change (Table 2). This finding is also directly relevant to clinical data, because any two patients with naturally differently-sized lungs that are administered the same amount of Technegas will have differences in contrast and information content of the SPECT

[3] We use the term information content in the strict sense of the number of grey values in an associated histogram that are non-zero.

recorded. Selecting textural parameters that are insensitive to this variability in data collection is an advantage in data interpretation.

Reconstructed SPECT data is routinely subjected to a rather strong smoothing filter before being presented to a radiographer or other medical professional. Filtering at the RNSH consists of a 9th order Butterworth filter with a cut-off of 1.2 cycles per centimetre. Since texture analysis by definition looks at small differences in grey values between pairs of pixels, any smoothing operation degrades the capabilities of the method for any given case. We tested this expected behaviour by preparing both simulated and normal patient data with and without applying the Butterworth filter and found the smoothed data set to have a poorer sensitivity as manifested in smaller relative changes in textural parameters. We will report the exact impact in a forthcoming separate study. In this work we only discuss reconstructed, extracted lung data that has **not** been subjected to any post-filtering.

A change of distance in the calculation of the GLCMs (within reason) adds little new information (Figure 1) with the exception of parameter TC2. In most cases the calculation of the GLCM for only one distance seems to be sufficient. For 2 of the textural parameters studied there is a better performance seen for shorter distances in the GLCM calculations (TC9 and TC30). This is plausible looking at the definitions (Appendix 1). Voxel pairs that are far from one another are unlikely to be highly correlated thus giving low correlation values in any lung (TC9) and uniformity between them will be near the random value (TC30).

From the simulated data it is known that $TC2_d$ drops with increasing defect size and in the patient data it drops with increasing NVV. This suggests that the average size of individual, non-ventilated areas increases with the severity of the diseases studied as opposed to a mere increase of number of non-ventilated areas of same size. This result is consistent with the perception of the SPECT data to the human eye.

Several well performing textural parameters were identified that by themselves allow to

distinguish between a 'normal' lung and a lung that suffers from some significant medical condition or disease. Combinations of textural parameters have the potential to further classify abnormal lungs. For example, to distinguish between asthmatics on one hand and COPD patients on the other hand one can combine the results from TC18 and the ratio TC30/TC31. TC18 is elevated in all diseases, but the ratio TC30/TC31 does not rise significantly in asthmatics while it does rise significantly in COPD patients (compare Figures 4 and 5).

Correlation of several key textural parameters with the corresponding ventilated lung volume are good to excellent for all patient data (Figures 6 and 7). Note that the ventilated lung volume is a measure that is calculated from the original imaging data (not the GLCM), while the FeV1 is a completely independent measurement. The pooling of data per disease group (Figures 4 and 5) combines all patients of one disease into one - independent of the severity of disease. Figures 6 and 7 on the other hand illustrate the relationship between reduced lung functionality and resulting changes in derived textural parameters. It is pointed out that reduced lung functionality goes along with higher heterogeneity in the SPECT data (Berend *et al.*, 2008) and textural parameters that measure heterogeneity increase while parameters that measure uniformity drop.

The textural parameters discussed are not all linearly independent of one another but some of them have substantial correlations amongst them. (Clausi, 2008). For practical matters it is desirable to identify a small number of textural parameters that give the overall best classification performance.

TC2, TC3, TC4 and TC30 are all measures of contrast, though with different weights. TC3 and TC30, which weigh values by the inverse of the contrast (homogeneity), have both shown consistently better performance in all patient data and either one of these two parameters are recommend for use. As TC3 and TC30 are highly correlated one should choose only one of them with TC3 performing marginally better in contrast-stretched data sets and TC30 better in

histogram-matched data sets.

TC1, TC21 and TC23 are all measures of orderliness. The ratio TC21/TC31 performed best in the clinical data. The GLCM Mean (TC31) reflects brightness changes between patients that the contrast-stretched data set is susceptible to. Thus using textural parameter combinations that involve the GLCM Mean improves correlation in several textural parameters studied. The histogram-matched data set shows no correlation with TC31 and combining textural parameters with TC31 carries no advantage and TC23 by itself gives the best performance in the group of textural parameters that measure orderliness. The value of Entropy (TC21, TC23) increases with increasing heterogeneity.

TC9 (Correlation), TC13 (Variance), TC18 (Coefficient of Variation) and TC31 (Mean) are descriptive statistics of the GLCMs and the frequency at which certain voxel *pairs* occur. The combination of Variance and Mean in the Coefficient of Variation (TC18) and the Variance over Mean ratio (TC13/TC31) gave excellent performance in the contrast-stretched data set and is another recommended parameter for use. TC18 and the TC13/TC31 ratio are highly correlated parameters. TC18 shows better correlation with ventilated lung volume and TC13/ TC31 shows better correlation with FeV1 but either one being a very good choice for characterising the clinical data.

GLCM Correlation (TC9) Is largely independent of the other texture measures and has the potential for giving additional insight. TC9 can be calculated for increasingly larger voxel distances and the size at which the value suddenly decreases is a measure for the size of definable objects in the original image data. However, we could not identify any 'sharp' drops but only gradual changes with the clinical data, suggesting that there is a broad size distribution of objects which makes this approach less powerful. Simply comparing the differences in Correlation values between the shortest and longest distance studied with ventilated lung volume resulted in a modest correlation (r^2=0.41).

It is noted that the best correlations between textural parameters and ventilated lung volume were achieved with a linear regression while correlation with FeV1 gave consistently better results using a logarithmic correlation function.

Summed up the following 3 recommendations can be made for the analysis of pulmonary SPECT-V data.

1) Texture analysis sensitivity is maximised by preparing SPECT data in an unfiltered, contrast-stretched way, as opposed to filtered or histogram-matched.

2) The choice of voxel pair distance in the GLCM calculation is non-critical. With present spatial resolution in SPECT data 1, 2, or 3 pixel distances are good choices that can also be pooled to improve statistics.

3) Amongst the many textural parameters studied one each should be chosen from 3 different groups of parameters to balance the capability to characterise with the computational effort involved. These are the textural parameters TC18 or the ratio TC13/TC31 from the descriptive statistics group, the parameter TC3 or TC30 from the contrast group and the parameter ratio TC21/TC31 in the orderliness group.

Application of the new software package is not limited to pulmonary studies – in fact it may also be applied to other organs or to completely different fields such as material sciences or mineralogy. However, in its present form the software package is optimized to the work-flow of studying lungs in a clinical scenario.

Summary

It has been demonstrated that a textural parameter analysis of functional pulmonary CT data has the potential to provide a robust and objective quantitative characterisation of

inhomogeneity in lung function and classification of lung diseases with application in routine clinical applications and national screening programmes. The new methods applied to SPECT lung ventilation scans are capable of distinguishing between different types of diseases. Strong correlations between key textural parameters and independent lung function data such as the FeV1 suggest that a quantitative description of the severity of diseases such as asthma or COPD by means of derived texture parameters is viable. Clear recommendations have been made for optimum data preparation and textural parameter selection. In a forthcoming study we plan to use data from larger numbers of patients and additional spirometry data to further refine the methods.

Acknowledgements

This work is supported by the Australian Research Council through the ARC Linkage Project LP0562715. The authors are grateful for scientific and technical input and support from the Australian Microscopy & Microanalysis Research Facility (AMMRF) node at the University of Sydney. We also like to thank the staff at the Royal North Shore Hospital that helped in the data collection and the volunteer patients that participated in this study. In particular we like to thank Peter Chicco, Department of Biomedical Engineering, who provided the lung simulations, Dale and Elizabeth Bailey, Department of Nuclear Medicine, for discussion and data conversion.

We like to thank Wayne Rasband and all other developers that made contributions to ImageJ and its plug-ins for sharing their work freely with other researchers (Rasband, 1997-2008, Abramoff *et al.*, 2004) – without them our work would have been much harder. Part of the software presented here started their development based on other publicly available plug-ins that are accessible through the ImageJ web page (Rasband,1997-2008, Castleman, 2005,

Miller, 2002).

References

Abramoff, MD, Magelhaes, PJ, Ram, SJ, Image Processing with ImageJ, Biophotonics International (2004), **11**(7)**:**36-42

Berend N, Salome CM, King GG, Mechanisms of airway hyper-responsiveness in asthma. Respirology (2008), **13**(5):624-631

Burger W and Burge MJ, Digital Image Processing - An Algorithmic Approach using Java. Springer-Verlag, New York (2008). ISBN 978-1-84628-379-6, www.imagingbook.com

Cabrera JE, "GLCM_Texture" plug-in for ImageJ, (2005), http://rsb.info.nih.gov/ij/plugins/

Castleman M, "Cell_outliner" plug-in for ImageJ (m@mlcastle.net), Columbia University (2005) http://rsb.info.nih.gov/ij/plugins/cell-outliner.html

Chicco P, Magnussen JS, Mackey DW, Bush V, Emmett L, Storey G, Bautovich G, and Wall H van der, SPET of a computerised model of diffuse lung disease, Eur.J.Nuc.Med (2001), **28**(2)**:**150-154

Choi HK, New Methods for Image Analysis of Tissue Sections. PhD thesis, Uppsala University, Sweden (1996), ISBN 91-554-3829-6

Clausi DA, An analysis of co-occurrence texture statistics as a function of grey level quantization. Can. J. Remote Sensing, (2002), **28**(1):45–62

Cradduck TD, Bailey DL, Hutton BF, Conninck F De, Busemann-Sokole E, Bergmann H, and Noelpp U, A standard protocol for the exchange of nuclear medicine image files. NucMedComm (1989), **10**:703-713

Downie SR, Salome CM, Verbanck S, Thompson BR, Berend N and King GG, Ventilation heterogeneity is a major determinant of airway hyperresponsiveness in asthma, independent of airway inflammation. Thorax (2007), **62**:684-689

Haralick RM, Shanmugam K, and Dinstein I, Textural features for image classification. IEEE Transactions on Systems, Man, and Cybernetics (1973), SMC-**3**(6):610-621

Haralick RM, Statistical and structural approaches to texture. Proceedings of the IEEE 67 (1979), **5**:786-804

Harris BE, Bailey D, Miles S, Bailey E, Rogers K, Roach P, Thomas P, Hensley M, and King GG, "Objective analysis of tomographic ventilation perfusion scintigraphy in pulmonary embolism", Am. J. Respir. Crit. Care Med. , March 15, 2007

Haynor DR, Harrison RL, Lewellen TK, The use of importance sampling techniques to improve the efficiency of photon tracking in emission tomography simulations. Med Phys (1991), **18**:990–1001

King GG, Eberl S, Salome CM, Meikle SR, and Woolcock AJ, Airway closure measured by a Technegas bolus and SPECT. Am.J.Respir.Crit.CareMed. (1997) **155**:682–688

King GG, Eberl S, Salome CM, Young IH, and Woolcock AJ, Differences in airway closure between normal and asthmatic subjects measured with single-photon emission computed tomography and technegas. Am.J.Respir.Crit.CareMed. (1998), **158**:1900–1906.

Lewellen TK, Anson CP, Haynor DR, Design of a simulation system for emission

tomographs. J Nucl Med (1988), **29**:871

Miller M, "Segmenting_Assistant", plug-in for ImageJ, (2002) mmiller3@iupui.edu, http://rsb.info.nih.gov/ij/plugins/index.html

Parker JA, Align3_TP: stack alignment plug-in for ImageJ, J.A.Parker@IEEE.org (version 25/Mar/2008), http://www.med.harvard.edu/JPNM/ij/plugins/Align3TP.html

Petersson J, Sánchez-Crespo A, Larsson SA and Mure M, Physiological imaging of the lung: single-photon-emission computed tomography (SPECT). J Appl Physiol (2007) **102**:468-476

Rasband, W.S., ImageJ, U. S. National Institutes of Health, Bethesda, Maryland, USA, http://rsb.info.nih.gov/ij/, 1997-2008.

Tgavalekos NT, Musch G,Harris RS, Vidal Melo MF, Winkler T, Schroeder T, Callahan R, Lutchen KR and Venegas JG, Relationship between airway narrowing, patchy ventilation and lung mechanics. Eur Respir J (2007), **29**:1174–1181

Venegas JG, Schroeder T, Harris S, Winkler RT, and Vidal Melo MF, The distribution of ventilation during bronchoconstriction is patchy and bimodal: A PET imaging study. Respiratory Physiology & Neurobiology (2005) **148**:57–64

WHO World Health Organisation, 2008a, http://www.who.int/respiratory/asthma/en/

WHO World Health Organisation, 2008b, http://www.who.int/respiratory/copd/en/

Xu J, Moonen M, Johansson Å, Gustafsson A, and Bake B, Quantitative analysis of inhomogeneity in ventilation SPET. Eur J Nucl Med (2001) **28**:1795–1800

Zubal IG, Harrell CR, Smith EO, Rattner Z, Gindi G, Hoffer PB, Computerized three-dimensional segmented human anatomy. Med Phys (1994), **21**:299–302

Appendix A: Definition of textural features from the co-occurrence matrix

A co-occurrence matrix P(i,j|d,θ) (PM for short) contains the probability that the grey level i occurs at a distance d in direction θ from a pixel with grey value j. N is the size of the co-occurrence matrix (N=256 in this study). Integrated sums are calculated from the matrix variance. We further define the vertical ($p_x(i)$), horizontal ($p_y(i)$), minor diagonal ($p_{x-y}(k)$) sums, the vertical (μ_x) and horizontal (μ_y) mean, and the variance of the vertical (V_x) and horizontal (V_y) directions (Choi, 1996). Note that the GLCM mean is distinct from the mean grey value of the original image because it is weighted by the frequency of occurrence *in combination with* a certain neighbour pixel value.

$P_x(i)=\Sigma_{j=0}^{N-1} PM$, $P_y(i)=\Sigma_{i=0}^{N-1} PM$, $P_{x-y}(k)=\Sigma_{i=0,|i-j|=k}^{N-1}\Sigma_{j=0}^{N-1} PM$, $\mu_x=\Sigma_i i\,P_x(i)$, $\mu_y=\Sigma_j j\,P_y(j)$, $V_x=\Sigma_i(i-\mu_x)^2 P_x(i)$, $V_y=\Sigma_j(j-\mu_y)^2 P_y(j)$

TC_1 Angular Second Moment $\Sigma_{i=0}^{N-1}\Sigma_{j=0}^{N-1} PM^2$

TC_2 Difference Moment or GLCM Contrast $\Sigma_{i=0}^{N-1}\Sigma_{j=0}^{N-1}(i-j)^2 PM$

TC_3 Inverse Difference Moment, $\Sigma_{i=0}^{N-1}\Sigma_{j=0}^{N-1}\left(1+(i-j)^2\right)^{-1} PM$

TC_4 Diagonal Moment, $\Sigma_{i=0}^{N-1}\Sigma_{j=0}^{N-1}\sqrt{0.5(i-j)PM}$

TC_7 Inertia, $\Sigma_{n=0}^{N-1} n^2\left(\Sigma_{i=0,|i-j|=n}^{N-1}\Sigma_{j=0}^{N-1}(i-j)^2 PM\right)$

TC_9 GLCM Correlation, $\left(\Sigma_{i=0}^{N-1}\Sigma_{j=0}^{N-1}(ij)PM-\mu_x\mu_y\right)/\sqrt{V_x V_y}$

TC13 GLCM Variance, V_x

TC18 Coefficient of Variation, $\sqrt{V_x V_y}/\mu_x\mu_y$

TC21 Entropy, $\Sigma_{i=0}^{N-1}\Sigma_{j=0}^{N-1}(PM)(-\ln(PM))$

TC23 Difference Entropy, $\Sigma_{i=0}^{N-1} P_{x-y}(i)\log_e\left(P_{x-y}(i)\right)$

TC30 Local Homogeneity. $\Sigma_{n=0}^{N-1}\left(P_{x-y}(n)/\left(1+n^2\right)\right)$

TC31 GLCM Mean $0.5\cdot(\mu_x+\mu_y)$

histogram	cube side length in [mm]	TC_1 Angular Second Moment	TC_3 Inverse Different Moment	TC_4 Diagonal Moment	TC_9 Correlation	TC18 Coefficient of Variation	TC21 Entropy	TC30 Local Homogeneity	TC13 Sum of squares / Variance	TC31 Mean	TC13/ TC31 Variance /Mean ratio
cs	2.5	111.9	4.2	-27.1	-15.2	22.5	-8.4	4.2	-2.2	-10.6	9.5
cs	5.0	106.4	7.5	-27.3	-20.0	28.9	-8.0	7.5	-16.8	-19.6	3.5
cs	7.5	85.8	9.0	-23.3	-22.3	46.6	-6.7	9.0	-17.7	-25.1	9.8
cs	10.0	68.6	10.5	-20.2	-19.2	77.0	-5.6	10.5	-15.6	-30.9	22.2
cs	**mean**	**93.2**	**7.8**	**-24.5**	**-19.2**	**43.7**	**-7.2**	**7.8**	**-13.1**	**-21.6**	**11.3**
hm	2.5	111.9	2.3	-27.2	-11.7	-0.7	-8.4	2.3	-0.4	0.1	-0.6
hm	5.0	106.4	-0.4	-24.9	-15.6	-0.1	-8.0	-0.4	-0.3	-0.1	-0.2
hm	7.5	85.8	0.4	-21.5	-16.1	-1.0	-6.8	0.4	-1.3	-0.2	-1.1
hm	10.0	68.6	2.1	-18.7	-13.8	0.1	-5.6	2.1	-1.1	-0.6	-0.5
hm	**mean**	**93.2**	**1.1**	**-23.1**	**-14.3**	**-0.4**	**-7.2**	**1.1**	**-0.8**	**-0.2**	**-0.6**

Table 1: Sensitivity of textural parameters to a 40% reduction in ventilated lung volume. The latter was achieved by randomly inserting black cubes of side length 2.5, 5, 7.5 and 10mm into the simulated lung. Results are shown as relative changes in the textural parameter for either preparing the data in a histogram-matched (hm) or a contrast-stretched (cs) way and as a mean over 5 distances used in the GLCM calculation.

Histogram	TC 1 Angular Second Moment	TC 3 Inverse Different Moment	TC 4 Diagonal Moment	TC 9 Correlation	TC18 Coefficient of Variation	TC21 Entropy	TC30 Local Homogeneity	TC13 Sum of squares (Variance)	TC31 Mean	TC13/ TC31 Variance /Mean ratio
cs	-62.6	-2.9	53.4	10.8	-10.8	11.5	-2.9	8.7	10.4	-1.5
hm	-62.3	-3.9	48.5	9.0	0.5	11.3	-3.9	-0.1	-0.3	0.2

Table 2: Sensitivity of textural parameters to a 40% increase in gamma counts. The simulated defects have a cube side length of 10mm. Listed are the differences in the values of the textural parameters derived from either the standard simulation with 40% NVV and associated drop in average brightness and an alternative simulation with a higher gamma count such that after knocking out 40% of the ventilated volume the IOD matched the IOD of the perfectly ventilated lung simulation.

Figure captions

Figure 1: *Illustration of textural parameter TC18, Coefficient of Variation, from the simulation study for cube-shaped defects of size 7.5mm cube side length as a function of non-ventilated lung volume in percent. The GLCMs were created for 5 pixel distances each (1, 2, 4, 8, 12 pixels) corresponding to distances in the lung of 4.7, 9.3, 18.7, 37.3 and 56.0mm, respectively. The coefficient of variation is larger for small pixel distances and increases with NVV and more rapidly so for larger defects (not illustrated).*

Figure 2: *Relative ventilated lung volume (solid black) and standard variation (hashed) per patient group.*

Figure 3: *Illustration of textural parameter TC18, the Coefficient of Variation, for a set of 5 'normal' lungs (left) and a set of 5 lungs of patients suffering from COPD (right). The severity of COPD increases from top to bottom.*

Figure 4: *Textural parameter 18 (solid black) and standard deviation (hashed) from the invariant GLCM and for all 5 distances for the 5 patient groups studied*

Figure 5: *Ratio of textural parameter 30/31 (solid black) and standard deviation (hashed) from the invariant GLCM and mean over 5 distances for the 5 patient groups studied*

Figure 6: *High correlation between ventilated lung volume in percent and textural parameter 18 (coefficient of variation) (r^2=0.955).*

Figure 7: *Correlation between textural parameter TC13/TC31 (Variance over Mean ratio) and independent spirometry data (FeV1) for 4 of the 5 patient groups. No spirometry data was available for the 'normal' group. The quality of the linear regression is r^2=0.66.*

FIGURE 1

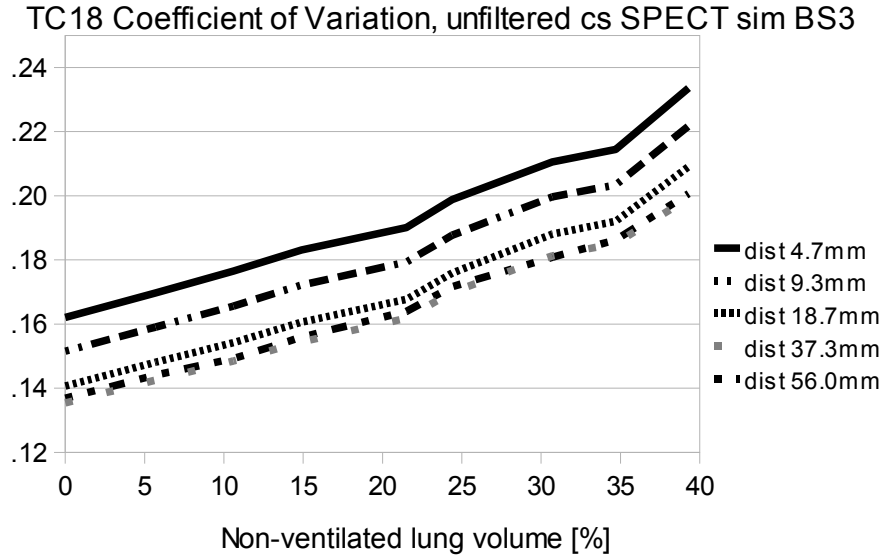

FIGURE 2

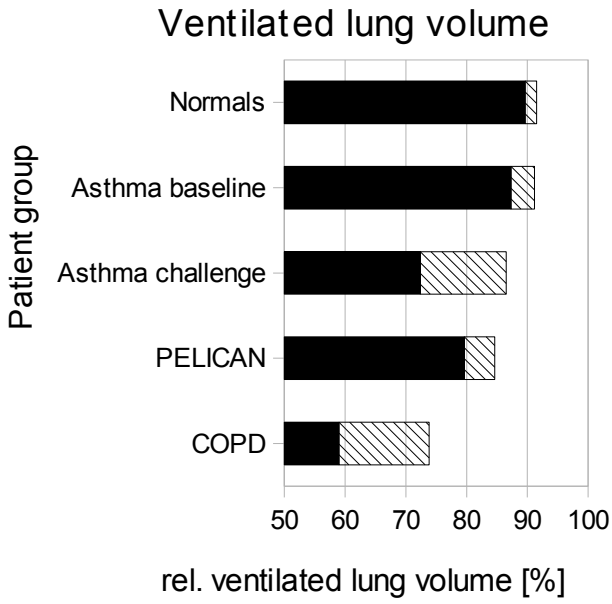

FIGURE 3 (left and right panel, reproduction in black-and-white)

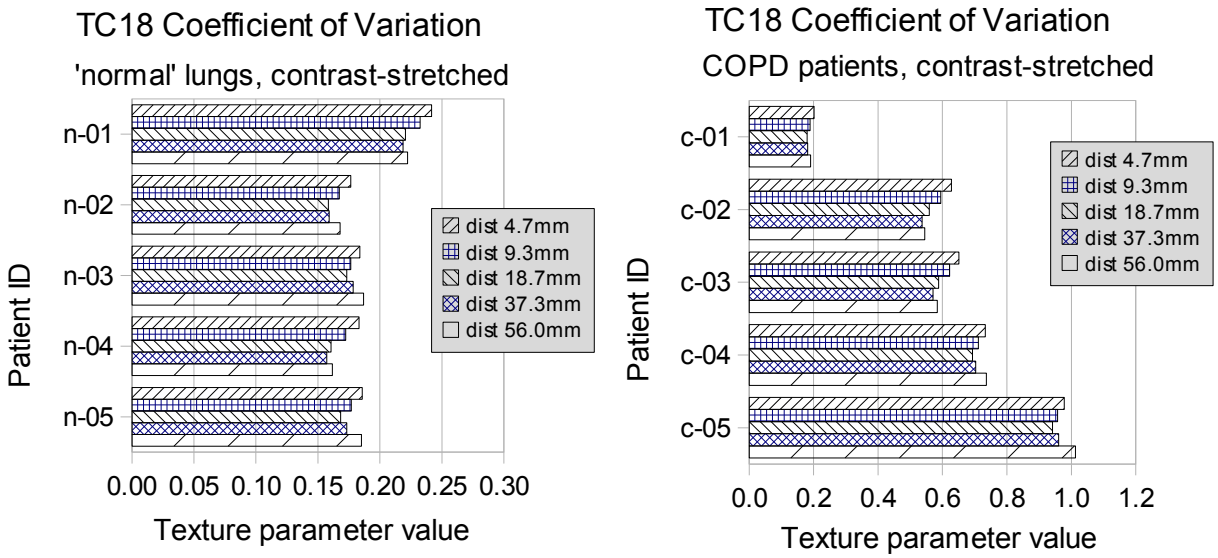

FIGURE 4

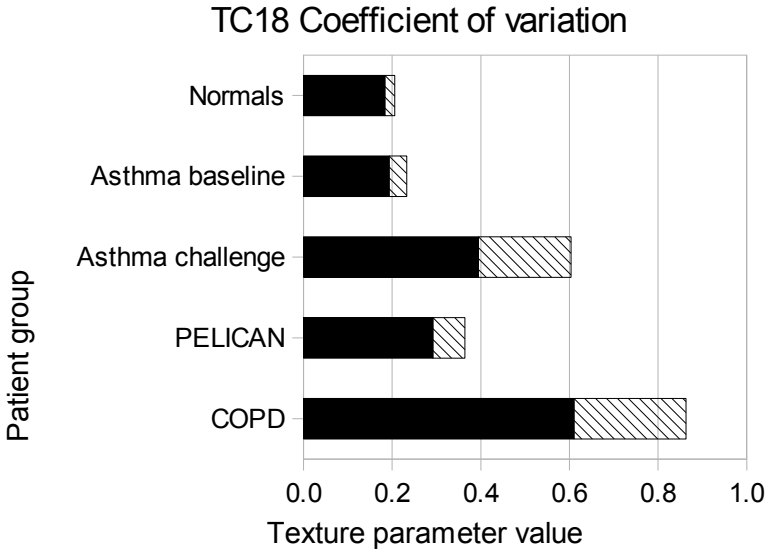

FIGURE 5

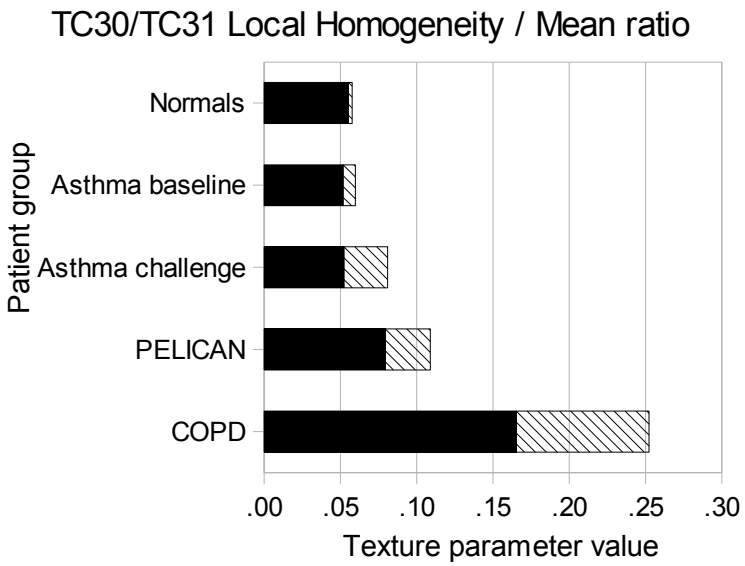

FIGURE 6 (colour reproduction for web-publishing, black-and-white for print)

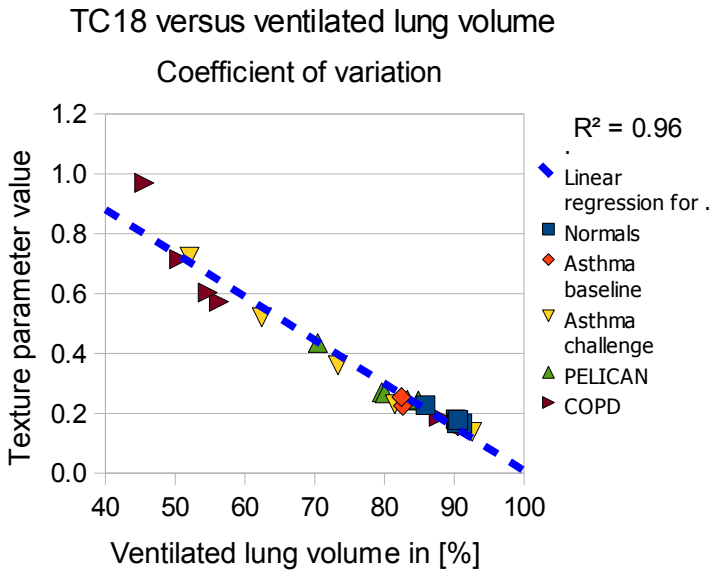

FIGURE 7 (colour reproduction for web-publishing, black-and-white for print)

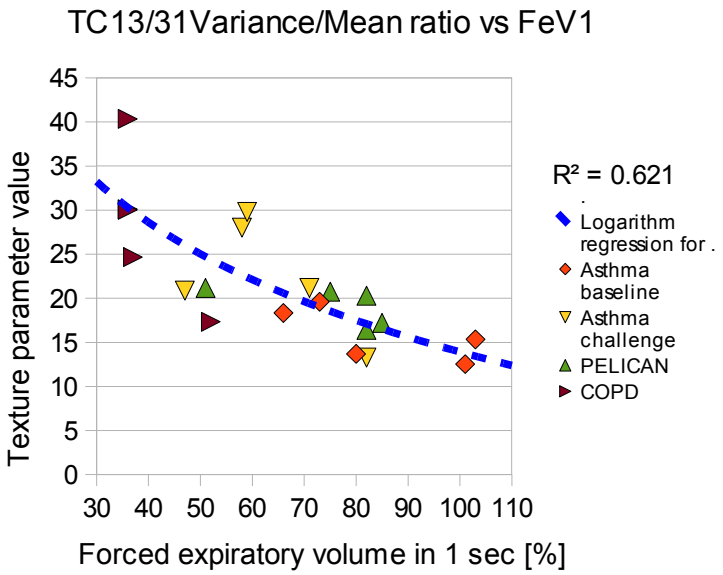

Application of Texture Analysis to Functional Pulmonary CT Data

Arndt Meier[a], Catherine Walsh[b,c,d], Benjamin E. Harris[b,c,d], Gregory G.King[b,c,d], and Allan Jones[a]

a) Australian Key Centre for Microscopy and Microanalysis, The University of Sydney, Sydney 2006, NSW, Australia, email: a.meier@usyd.edu.au *(corresponding author)*

b) Department of Respiratory Medicine, Royal North Shore Hospital, St Leonards NSW 2065

c) Woolcock Inst. of Medical Research, 431 Glebe Point Road, Glebe, NSW 2037

d) Northern Clinical School, Faculty of Medicine, University of Sydney, Sydney, 2006

Abstract

It is demonstrated that textural parameters calculated from functional pulmonary CT data have the potential to provide a robust and objective quantitative characterisation of inhomogeneity in lung function and classification of lung diseases in routine clinical applications. Clear recommendations are made for optimum data preparation and textural parameter selection.

A new set of platform-independent software tools are presented that are implemented as plug-ins for ImageJ. The tools allow segmentation and subsequent histogram-based and grey-level co-occurrence matrix based analysis of the regions of interest. The work-flow is optimised for use in a clinical environment for the analysis of transverse Computed Tomography (CT) scans and lung ventilation scans based on SPECT. Consistency tests are made against other texture analysis plug-ins and simulated lung CT data. The same methods are then applied to patient data consisting of a healthy reference group and one patient group each who suffered from asthma, chronic obstructive pulmonary disease (COPD), and COPD plus lung cancer. The potential for disease classification based on computer analysis is evaluated.

KEYWORDS:

texture analysis, computed tomography, asthma, COPD, lung ventilation

1. Introduction

Close to 10 percent of the world population are suffering from chronic lung diseases. The two most common categories, which account for 7.7%, are asthma and chronic obstructive pulmonary disease (COPD).

According to World Health Organisation (WHO) estimates, 300 million people suffer from asthma and 255 000 people died of asthma in 2005 (WHO, 2008a) and an increase of 20% is expected over the next 10 years. Asthma is the most common chronic disease among children. It is characteried by episodic airway narrowing that occurs on exposure to stimuli, such as exercise, dust, pollens and cold air. Asthmatic lungs are characterised by inhomogeneous ventilation when studied by pulmonary function techniques or by imaging methods. The severity of the inhomogeneity, measured by pulmonary function, is strongly related to the sensitivity of airways to inhalants, i.e. dust, pollens etc. Thus characterisation of the topographical pattern of ventilation in asthmatic lungs is important

The WHO estimates (2007), currently 210 million people suffer from chronic obstructive pulmonary disease (COPD) with 3 million people dying of COPD in 2005 (WHO, 2008b). COPD is a chronic disease that is caused predominantly by tobacco smoking in western countries. COPD causes lung destruction, known as emphysema, and diseases of small and large airways, which result in cough, mucous production and airway narrowing with resultant breathlessness during exertion.

Single-photon emission computed tomography (SPECT) ventilation scanning (Petersson *et al.*, 2007) using Technetium-99 (Technegas^{TM}), is a three dimensional imaging technique used routinely in clinical nuclear medicine for diagnosis of diseases such as pulmonary embolism, when combined with imaging of blood flow (Harris *et al.*, 2007). Ventilation scans, however, have been adapted for studies of ventilation in airways disease (King *et al.,* 1997 and 1998,

Downie *et al.*, 2007). SPECT imaging offers the potential to characterise the topographical distribution of ventilation so that inhomogeneity can be quantified at the regional level (Xu *et al.*, 2001, Venegas *et al.*, 2005). Combining imaging information with the pulmonary function measures of inhomogeneity will provide important information about the ventilatory abnormalities in asthma and COPD (Tgavalekos *et al.,* 2007, Berend *et al.*, 2008). However, suitable methods for quantifying the distribution of ventilation from SPECT data have not been determined.

In this study, we investigate several potentially useful methods of quantifying the distribution of ventilation from SPECT ventilation data using both simulated SPECT data and data from well-described clinical groups. The new technique is based on texture analysis and can provide an objective indicator of abnormal lung conditions.

2. Methods

We developed new techniques for multiple 3D texture analysis and conventional 3D image analysis of clinical SPECT data of volumes representing lung tissue as identified from co-registered CT scans that were obtained at the time of the SPECT.

The new technique uses the anatomical CT to define the lung outlines, co-registers these with the functional SPECT data and performs an image analysis on the voxels of the SPECT thus defined as representing lung tissue. The image analysis comprises a traditional direct analysis of the grey levels in the SPECT slices and a texture parameters analysis derived from grey-level co-occurrence matrices (GLCM) (Haralick, *et al.*, 1973, Choi, 2006).

2.1 Simulation data

We created a series of SPECT-V data sets based on simulated data to validate the software. The lung phantom used in the construction of the model was based upon X-ray computed tomography (CT) data from a male of height 178 cm, weighing 70 kg (Zubal *et al.*, 1994) in supine position, who was chosen for his similarity to the dosimetry standard mathematical phantom. The Monte Carlo simulation package used for this work was the Photon History Generator (Lewellen *et al.*, 1988, Haynor *et al.*,1991), which models the emission, scatter and attenuation of photons in a heterogeneous phantom, followed by the photons' subsequent collimation and detection (Chicco *et al.*, 2001).

Simulations were performed for a 23.6-mm-thick parallel-hole collimator, using a 32.5-cm radius of rotation. The isotope modelled was Tc99, collected with a symmetric 20% energy window centred around 140 keV into a 128×128 matrix with 120 views at equal angular spacing around 360°, resulting in 5 million counts total when no defects were present. Pixel resolution was 2.5mm/pixel. To test for any dependence on brightness changes we repeated two simulations with 9 million counts. These settings were chosen to closely mimic typical clinical settings when collecting SPECT-V data (similar contrast, spatial resolution and signal to noise).

A series of studies were performed in four groups, distinguished by the size of individual defects, to simulate the effects of non-ventilated lung tissue. Defects in groups 1–4 were 1x1x1 pixels (15 mm^3), 2x2x2 pixels (125 mm^3), 3x3x3 pixels (422 mm^3) and 4x4x4 pixels (1000 mm^3) in size, respectively. These were distributed uniformly throughout both lung halves in a random manner. Within each group, the amount of lung tissue involved in defects varied from 0% (normal) up to 40% in steps of 5%, giving 9 studies in each group.

These simulated lung data sets were then subjected to normal clinical processing. Lungs were reconstructed at the same resolution as routine SPECT data (128 slices with 128x128 pixels, voxel size 4.664mm^3). The lung outlines were known from the original phantom and

converted to a binary mask which was then subjected to 2 iterations with the standard ImageJ erosion operation using a count of 3 (minimum 3 of the nearest neighbour pixels need to be background pixels for the present pixel to be eroded).

2.2 Clinical data

Three groups of patients were studied to evaluate the applicability of the new methods. Five patients had asthma (data set A), and 10 current or ex-smokers that had either diagnosed COPD (data set C) or were being evaluated for treatment of lung cancer (PELICAN[1] data set) who had a wide range of severity of COPD, and scans from 5 patients who underwent lung scanning for suspected pulmonary embolism but who were considered to have normal lung scans on routine clinical assessment (data set N).

All subjects inhaled Technegas as the ventilation imaging agent. Patients had scans according to the standard clinical protocol whereby Technegas was inhaled from the Technegas generator by 1-2 deep inspirations followed by a breath hold to maximise Technegas particle deposition.

Subjects had a ventilation SPECT scan and a CT scan acquired by a dual-detector variable angle hybrid SPECT/CT system (Phillips SKYLight and Picker PQ5000 CT). All SPECT studies were acquired using a 128 x 128 matrix, at 15 seconds per stop with 3 degree steps over 360 degrees. Low-dose CT was performed using non-contrast (30mA, 10kVp, pitch 1.5, slice thickness 4mm). Study was acquired during tidal breathing. CT images are reconstructed using a 512 x 512 matrix with a smooth algorithm.

Spirometry, including the predicted forced experitory volume during one second (FeV1), was

[1] PELICAN study: Predicting Exercise tolerance and Lung function using Imaging in patients undergoing CANcer Surgery, Royal North Shore Hospital, internal study, 2007.

obtained in all groups except the normal group, using standard methods in the lung function laboratory.

2.3 Software

Custom plug-ins were developed for ImageJ (Rasband, 1997-2008) to read and write CT data routinely stored in Interfile data format (Cradduck et al., 1989). Segmentation of the lungs in the CT datasets is done with a custom written plug-in "Extract_Lungs", which was more efficient than existing segmentation plug-ins (Parker, 2008, Castleman, 2005). Segmentation uses an edge-following algorithm that stays between an upper and lower grey-value threshold. If the initial seed-point falls outside the thresholds, a new seed-point is automatically determined from a search towards the median point of the previous slice and an outward spiral from there if that fails.

Up to 5 regions of interest per slice are supported which are categorised as belonging to either the left or right lungs. A custom-built ROI manager allows superimposition of the ROIs onto SPECT ventilation data. The identified volumes are analysed for total area, mean, median, modal, minimum, and maximum grey values, kurtosis, integrated optical density (IOD), and histogram. Weighted means are calculated for left, right and total lung.

Anatomical CT data were registered to corresponding functional data (SPECT) with the ImageJ plug-in Align3_TP (Parker, 2008) with all parameters left to their default values. The outlines of the registered lung mask were then auto-detected with our segmentation algorithm resulting in ImageJ standard ROIs (regions of interest). Our modified ROI manager limits all subsequent analysis to within the defined ROIs.

From these ROIs that represent the total lung volume, GLCMs are calculated for the x, y, z, and invariant orientation for a set of up to 5 chosen distances. These are then subjected to

standard texture analysis. We verified the correct implementation of the GLCM algorithm by comparing results from an independently written plug-in [Cabrera, 2005], which calculates 4 of the 12 textural features we determine, and found both to be consistent.

Our methods are based on software that is easily available, widely used, modular in design, open source and not limited to a specific operating system. ImageJ (Rasband, 1997-2008), Abramoff *et al.*, 2004, Burger & Burge, 2008) fulfils all these criteria perfectly. And more so, there is a very large collection of plug-ins publicly available (http://rsb.info.nih.gov/ij/plugins/). The code used in this study is available from the author.

2.4 Analysis

In both the simulated and the clinical data the volumes representing lung tissue were identified as described above. All voxels outside the eroded ROIs were excluded from the analysis. Note that lung tissue outlines were registered to the reconstructed SPECT data, thus avoiding any interpolation in the SPECT data set.

All SPECT data sets, simulated and clinical, were prepared in two parallel streams: *CS* (contrast stretched) and *HM* (histogram matched). The contrast stretched data set was created by first stretching the contrast within the 16-bit grey-levels image stack using the stack histogram (built-in ImageJ function) and then converting the image stack to an 8-bit grey-level image stack. The latter step used an improved version of the ImageJ Stack Converter that uses the stack histogram as opposed to the histogram of the current slice and allows to fold a set percentage of hot pixels into the highest remaining histogram channel. We chose the 0.02% brightest non-background pixels to be treated as hot pixels.

The histogram-matched data set used the histogram from the best ventilated simulated lung as the reference histogram after smoothing it twice with a Gaussian filter of 5 histogram

channels width. This histogram compared well with histograms obtained from patients with normal lung function. The histogram matcher we wrote uses the stack histogram and can directly map a 16-bit image stack onto an 8-bit reference histogram thus considerably reducing channel pile-up effects commonly encountered when first converting from 16-bit to 8-bit and then again from 8-bit to 8-bit reference histogram.

The 'extracted lungs' as defined by sets of ROIs were then analysed in two steps. The normal grey value analysis calculated the total lung volume in voxels, the ventilated volume, the minimum, mean, modal, median and maximum grey values, IOD, contrast, histogram, and Kurtosis on a per-ROI basis. Mean values weighted by ROI area were calculated for left, right, and total lung.

A voxel was considered to represent ventilated lung tissue if it had a grey value larger than 20% of the histogram maximum. To minimise the impact of any erratic hot pixels, the histogram maximum was calculated from the 97% level assuming that the histogram above 97% drops with a slope of -0.5. In this work we only report the results for total lungs, but it is noted that the software reports more details where this may be of interest.

The second step of the analysis created 8-bit grey-level co-occurrence matrices (GLCMs) from all the ROIs of any one lung for 5 distances each: 1, 2, 4, 8, and 12 pixels (4.7, 9.3, 18.7, 37.3, 56.0mm) and for 4 direction pairs each: X (left->right, right->left), Y (top->bottom, bottom->top), Z (up->down, down->up) and I (invariant, combining X, Y, and Z). The invariant matrix we chose gives equal weight to each valid voxel pair and may at times differ from a mean over the X, Y, and Z matrices as individual matrices may not have the exact same number of voxel pairs. From these GLCMs twelve texture features were calculated as listed in appendix A (Haralick *et al.*, 1973, Haralick 1979, Choi, 1996).

3. Results

3.1 Results from the phantom study

The texture parameters calculated from the simulated lungs show a number of correlations with the size of the defects and the total non-ventilated volume (NVV). Figure 1 illustrates this for the example of the textural parameter TC18 (coefficient of variation) and simulated defect sizes of 3x3x3 pixels. For all GLCM distances and defect sizes the parameter TC18 increases steadily with increasing NVV and more rapidly so for larger defects.

No significant differences were found between results obtained from X, Y, and Z GLCMs. Hence only the invariant GLCMs have been studied further. For all 12 textural parameters studied we found under all conditions that the functions such as in Figure 1 are smooth and steady and that different distances in GLCM calculation result in slightly shifted versions of the same shape but that in no case does the graph of one distance cross the graph of another distance for otherwise identical settings. On the contrary, we often saw that graphs for different distances were almost undistinguishable from one another. Consequently the data from all distances were pooled into one; thus reducing the complexity of the results presented. Notwithstanding this, it is noted, that TC9 and TC30 were somewhat more sensitive to NVV changes at shorter distances and that TC2 showed no dependence on NVV but gave significantly different results for different distances.

For clarity only the relative changes in textural parameters between the lowest and highest NVV studied are reported, because the functions change smoothly with NVV and in-between values do not add much to the discussion.

Table 1 lists the relative changes in the textural parameters calculated in response to a 40% drop in ventilated lung volume. Some textural parameters are more sensitive to the changes in ventilated volume than others as can be seen from Table 1 (rows 6 and 11 "*mean*"). Also,

they are typically stronger in the contrast-stretched data set (***cs***, row 6) as compared to the histogram-matched data set (***hm***, row 11).

The results from a sensitivity test to brightness changes are shown in Table 2. We repeated the simulation for the "worst" lung with a higher activity such that after adding the defects it resulted in the same IOD as the perfectly ventilated simulated lung. Insensitivity to brightness changes would allow the direct comparison of textural parameters derived from studies that use different gamma counts. Note that rows 2 and 3 in Table 2 correspond to rows 5 and 10 in Table 1 (10 mm), respectively, but the percentage changes are expressed relative to the values in Table 1. It is noted that the sign of all values in Table 2 act in such a way as to reduce the sensitivity of the textural parameters.

In the context of our work a good textural parameter is one that is sensitive to changes in NVV or defect-size and that is at the same time insensitive to changes in brightness. With this in mind we can group the textural parameters investigated into robust, intermediate and poor performers:

Robust textural parameters:

TC13/TC31 Variance/Mean ratio: provides a solid signal of 22% change in the parameter value for a 40% change in NVV while its dependence on brightness doubling is only small (1.5%). The sensitivity is somewhat poorer for smaller defects.

TC30 Local homogeneity: provides still a good signal of 10.5% change for a 40% drop in NVV but is more sensitive to brightness changes than the TC13/TC31 ratio (2.9%).

TC18 Coefficient of Variation: provides a very strong signal of 77% for large defects and a still strong signal of 22% for small defects. It has a moderate dependence on brightness changes (10.8% simulating large defects). However, correlation with clinical data discussed

below is excellent.

Textural parameters with intermediate performance:

TC1 Angular second moment: provides high sensitivity (>68%) to changes in NVV, but unfortunately it is also very sensitive to brightness changes.

TC2 and TC2: Difference and inverse difference moment: show a modest sensitivity for short distances and small-sized defects but are insensitive at larger pixel distances as well as for larger defect sizes. However, they may be used successfully in conjunction with other parameters to decide whether the effective size distribution of the non-ventilated volumes is small or large.

TC9 Correlation: The theoretical study shows a reasonable sensitivity of around 20% to changes twice that large in NVV but also a relatively high sensitivity to brightness changes. In the clinical studies discussed below this parameter did not convince and is outperformed by others.

Textural parameters with poor performance:

TC7, TC4, TC13, TC31, TC21, and TC23: These parameters suffer either from a lack of sensitivity or high sensitivity to changes in brightness.

Combination of textural parameters:

The ratio of TC13/TC31 is a very good performer although neither TC13 nor TC31 are good performers. Similarly, the ratio of TC21/TC31 gives a moderately good performance.

3.2 Results from the clinical studies

Figure 2 illustrates the estimated ventilated lung volume grouped by patient group. The 'normal' group shows the highest ventilated volume of about 90% and the smallest variance. Asthmatic lungs at baseline show a slightly lower ventilated lung volume although not statistically significant from the 'normal' lungs. The remaining patient groups show significant reductions in ventilated lung volume that are strongest in COPD patients. There is also a higher variability in these groups.

Figures 3 and 4 illustrate one of the best performing textural parameters for the 5 patient groups studied. Both the absolute value and the variability between different GLCM distances and between patients in the 'normal' lung function group are small (Figure 3, left panel). The results from COPD patients which range from a mild case (right panel, c-01) to severe (c-05) show increasingly higher values.

The differences between using different distances in the GLCM calculations are almost within the numerical precision, which was also observed in the results from the simulated data. This observation holds true for all textural parameters and patient groups studied except for TC2, TC9 and TC30. TC9 (Correlation) and TC30 (Local Homogeneity) lose sensitivity with increasing distance between voxel pairs and better performance is achieved by only using the 2 shortest distances (1 and 2 pixels distance corresponding to 4.7 and 9.3mm, respectively). TC2 will be discussed separately below. These findings are consistent with observations from the simulated data.

Pooling the data from all GLCM distances[2] and by patient group allows us to look for disease-specific differences as shown in Figure 4.While asthmatics at baseline cannot be distinguished from normal lungs, they can be clearly identified after a Metacholine challenge. PELICAN patients and even more so COPD patients have strongly elevated values in the coefficient of

[2] Except for TC9 and TC30 which pooled only the 2 shortest distances for higher sensitivity

variation calculated from the GLCM.

Figure 5 presents the ratio of Local Homogeneity and GLCM Mean (TC30/TC31) calculated in the same way as in the previous figure. Again, values for COPD and PELICAN patients are significantly higher than those for normal and asthmatic lungs. It is noted, however, that asthma patients both at baseline and at Metacholine challenge give almost identical results. Hence combining the information from multiple textural parameters allows to distinguish between different disease classes such as asthma from COPD.

A very strong correlation (r^2=0.955) between the textural parameter Coefficient of Variation (TC18) and the estimated ventilated lung volume is illustrated in Figure 6. Similarly high correlations of r^2>0.8 exist for textural parameters TC3, TC30, TC31, and the ratios TC13/TC31 and TC21/TC31 as a function of ventilated lung volume (not illustrated). More positive correlations (r^2>0.49) are observed for textural parameters TC1, TC9, and the ratio TC1/TC31.

Independent spirometry data in the form of the predicted forced expiratory volume during 1 second (FeV1) was available for all but the 'normal' group. Again good correlations are observed with several textural parameters (r^2 >0.5 for TC18 and TC13/TC31, r^2 >0.4 for TC3, TC30, TC21/TC31, TC31 and TC1/TC31 and r^2 >0.3 for TC1, TC2 and TC9) as illustrated in Figure 7 for the example of TC13/TC31.

The Difference Moment (TC2) behaves differently from all other textural parameters studied. It is insensitive to changes in both NVV and FeV1, but it is sensitive to the size distribution of patterns in the lung. Hence the TC2 textural parameter results were prepared in a different way. Instead of pooling the results from different GLCM distances, the parameter value obtained with the shortest distance (1 pixel) were divided by the parameter value for the second largest distance for any one lung and that we refer to as $TC2_d$ for short. Data prepared in this way resulted in a positive correlation of $TC2_d$ with NVV (r^2 =0.69) and a somewhat

weaker correlation with FeV1 (r^2 =0.375).

All results in this section were derived from the contrast-stretched data set as it showed an overall better performance than compared to results derived from the histogram-matched data. It is noted that TC18, TC31 (Mean) and TC13/TC31 were indifferent to both NVV and FeV1 changes in the histogram-matched data set, but otherwise the same textural parameters performed well as in the contrast-stretched data set. The only textural parameter that faired significantly better in the histogram-matched data set was TC23 (Difference Entropy).

4 Discussion

Changes in the grey level distribution such as a shift to darker grey values – as can be expected with a reduction in ventilated lung volume – is essentially removed in the histogram-matched data. Hence, changes in the textural parameters that occur in the contrast-stretched data set but not in the histogram-matched one are thought to be driven by histogram changes while changes that occur in the histogram-matched data set are thought to be dominated by changes in pattern (Table 1). Changes in the contrast-stretched data set are often a result of both histogram and pattern changes.

In an ideal system a change in brightness should not affect the textural parameters calculated because the GLCMs are always normalised to an IOD of unity. However, it is noted that the spatial resolution of the observation system is significantly lower than the features that cause them. The effective resolution in the SPECT-V data is lower than the pixel resolution of 4.664mm/pxl which in turn is much coarser than the simulated small defects starting from 2.5mm cube side length. Due to the nature of discrete sampling – and in this case significant under-sampling – of the object space and the non-linearity of the resulting effective blurring, the texture parameters calculated become dependent on the total optical density and contrast

in the SPECT-V data sets. This effect itself is also dependent on the effective size distribution of the defects we seek to describe. To quantitatively describe the exact relationship is mathematically complex and of limited practical use as it will vary from situation to situation. Instead we seek to identify textural parameters that depend acceptably little on the variability in patient data preparation.

The simulated data allows to fully control the environment, to know the true size distribution of the non-ventilated lung volumes, the true ventilated volume, and to vary some of these parameters systematically to study its impact. However, there are also some differences and limitations compared to clinical data that are undesirable. One is that the IOD of the simulated SPECT-V scan drops progressively with increasing NVV due to the simplicity of the model available to us.

A patient with a smaller ventilated lung volume inhales approximately the same amount of radioactivity as a patient with a larger ventilated lung volume. As a result the scan from the former patient would have a larger information content3 and image contrast; because the same amount of activity has to squeeze into a smaller volume, a wider range of different brightness values is observed. Hence a poorly ventilated *simulated* lung has a somewhat *lower* information content in the simulated data in contrast to a patient with a poorly ventilated lung that would result in a *higher* information content than the ideally ventilated lung. We studied this behaviour by simulating one data set with a higher gamma count, which resulted in an increase of 38% in information content as opposed to a 9% drop in the non-corrected simulation case. Although the textural parameters are modified as a result, it does not change the overall response to NVV and we were able to identify textural parameters that are little or non-susceptible to this change (Table 2). This finding is also directly relevant to clinical data, because any two patients with naturally differently-sized lungs that are administered the same

[3] We use the term information content in the strict sense of the number of grey values in an associated histogram that are non-zero.

amount of Technegas will have differences in contrast and information content of the SPECT recorded. Selecting textural parameters that are insensitive to this variability in data collection is an advantage in data interpretation.

Reconstructed SPECT data is routinely subjected to a rather strong smoothing filter before being presented to a radiographer or other medical professional. Filtering at the RNSH consists of a 9^{th} order Butterworth filter with a cut-off of 1.2 cycles per centimetre. Since texture analysis by definition looks at small differences in grey values between pairs of pixels, any smoothing operation degrades the capabilities of the method for any given case. We tested this expected behaviour by preparing both simulated and normal patient data with and without applying the Butterworth filter and found the smoothed data set to have a poorer sensitivity as manifested in smaller relative changes in textural parameters. We will report the exact impact in a forthcoming separate study. In this work we only discuss reconstructed, extracted lung data that has **not** been subjected to any post-filtering.

A change of distance in the calculation of the GLCMs (within reason) adds little new information (Figure 1) with the exception of parameter TC2. In most cases the calculation of the GLCM for only one distance seems to be sufficient. For 2 of the textural parameters studied there is a better performance seen for shorter distances in the GLCM calculations (TC9 and TC30). This is plausible looking at the definitions (Appendix 1). Voxel pairs that are far from one another are unlikely to be highly correlated thus giving low correlation values in any lung (TC9) and uniformity between them will be near the random value (TC30).

From the simulated data it is known that $TC2_d$ drops with increasing defect size and in the patient data it drops with increasing NVV. This suggests that the average size of individual, non-ventilated areas increases with the severity of the diseases studied as opposed to a mere increase of number of non-ventilated areas of same size. This result is consistent with the perception of the SPECT data to the human eye.

Several well performing textural parameters were identified that by themselves allow to distinguish between a 'normal' lung and a lung that suffers from some significant medical condition or disease. Combinations of textural parameters have the potential to further classify abnormal lungs. For example, to distinguish between asthmatics on one hand and COPD patients on the other hand one can combine the results from TC18 and the ratio TC30/TC31. TC18 is elevated in all diseases, but the ratio TC30/TC31 does not rise significantly in asthmatics while it does rise significantly in COPD patients (compare Figures 4 and 5).

Correlation of several key textural parameters with the corresponding ventilated lung volume are good to excellent for all patient data (Figures 6 and 7). Note that the ventilated lung volume is a measure that is calculated from the original imaging data (not the GLCM), while the FeV1 is a completely independent measurement. The pooling of data per disease group (Figures 4 and 5) combines all patients of one disease into one - independent of the severity of disease. Figures 6 and 7 on the other hand illustrate the relationship between reduced lung functionality and resulting changes in derived textural parameters. It is pointed out that reduced lung functionality goes along with higher heterogeneity in the SPECT data (Berend *et al.*, 2008) and textural parameters that measure heterogeneity increase while parameters that measure uniformity drop.

The textural parameters discussed are not all linearly independent of one another but some of them have substantial correlations amongst them. (Clausi, 2008). For practical matters it is desirable to identify a small number of textural parameters that give the overall best classification performance.

TC2, TC3, TC4 and TC30 are all measures of contrast, though with different weights. TC3 and TC30, which weigh values by the inverse of the contrast (homogeneity), have both shown consistently better performance in all patient data and either one of these two parameters are

recommend for use. As TC3 and TC30 are highly correlated one should choose only one of them with TC3 performing marginally better in contrast-stretched data sets and TC30 better in histogram-matched data sets.

TC1, TC21 and TC23 are all measures of orderliness. The ratio TC21/TC31 performed best in the clinical data. The GLCM Mean (TC31) reflects brightness changes between patients that the contrast-stretched data set is susceptible to. Thus using textural parameter combinations that involve the GLCM Mean improves correlation in several textural parameters studied. The histogram-matched data set shows no correlation with TC31 and combining textural parameters with TC31 carries no advantage and TC23 by itself gives the best performance in the group of textural parameters that measure orderliness. The value of Entropy (TC21, TC23) increases with increasing heterogeneity.

TC9 (Correlation), TC13 (Variance), TC18 (Coefficient of Variation) and TC31 (Mean) are descriptive statistics of the GLCMs and the frequency at which certain voxel *pairs* occur. The combination of Variance and Mean in the Coefficient of Variation (TC18) and the Variance over Mean ratio (TC13/TC31) gave excellent performance in the contrast-stretched data set and is another recommended parameter for use. TC18 and the TC13/TC31 ratio are highly correlated parameters. TC18 shows better correlation with ventilated lung volume and TC13/TC31 shows better correlation with FeV1 but either one being a very good choice for characterising the clinical data.

GLCM Correlation (TC9) Is largely independent of the other texture measures and has the potential for giving additional insight. TC9 can be calculated for increasingly larger voxel distances and the size at which the value suddenly decreases is a measure for the size of definable objects in the original image data. However, we could not identify any 'sharp' drops but only gradual changes with the clinical data, suggesting that there is a broad size distribution of objects which makes this approach less powerful. Simply comparing the

differences in Correlation values between the shortest and longest distance studied with ventilated lung volume resulted in a modest correlation (r^2=0.41).

It is noted that the best correlations between textural parameters and ventilated lung volume were achieved with a linear regression while correlation with FeV1 gave consistently better results using a logarithmic correlation function.

Summed up the following 3 recommendations can be made for the analysis of pulmonary SPECT-V data.

1) Texture analysis sensitivity is maximised by preparing SPECT data in an unfiltered, contrast-stretched way, as opposed to filtered or histogram-matched.

2) The choice of voxel pair distance in the GLCM calculation is non-critical. With present spatial resolution in SPECT data 1, 2, or 3 pixel distances are good choices that can also be pooled to improve statistics.

3) Amongst the many textural parameters studied one each should be chosen from 3 different groups of parameters to balance the capability to characterise with the computational effort involved. These are the textural parameters TC18 or the ratio TC13/TC31 from the descriptive statistics group, the parameter TC3 or TC30 from the contrast group and the parameter ratio TC21/TC31 in the orderliness group.

Application of the new software package is not limited to pulmonary studies – in fact it may also be applied to other organs or to completely different fields such as material sciences or mineralogy. However, in its present form the software package is optimized to the work-flow of studying lungs in a clinical scenario.

Summary

It has been demonstrated that a textural parameter analysis of functional pulmonary CT data has the potential to provide a robust and objective quantitative characterisation of inhomogeneity in lung function and classification of lung diseases with application in routine clinical applications and national screening programmes. The new methods applied to SPECT lung ventilation scans are capable of distinguishing between different types of diseases. Strong correlations between key textural parameters and independent lung function data such as the FeV1 suggest that a quantitative description of the severity of diseases such as asthma or COPD by means of derived texture parameters is viable. Clear recommendations have been made for optimum data preparation and textural parameter selection. In a forthcoming study we plan to use data from larger numbers of patients and additional spirometry data to further refine the methods.

Acknowledgements

This work is supported by the Australian Research Council through the ARC Linkage Project LP0562715. The authors are grateful for scientific and technical input and support from the Australian Microscopy & Microanalysis Research Facility (AMMRF) node at the University of Sydney. We also like to thank the staff at the Royal North Shore Hospital that helped in the data collection and the volunteer patients that participated in this study. In particular we like to thank Peter Chicco, Department of Biomedical Engineering, who provided the lung simulations, Dale and Elizabeth Bailey, Department of Nuclear Medicine, for discussion and data conversion.

We like to thank Wayne Rasband and all other developers that made contributions to ImageJ and its plug-ins for sharing their work freely with other researchers (Rasband, 1997-2008, Abramoff *et al.*, 2004) – without them our work would have been much harder. Part of the

software presented here started their development based on other publicly available plug-ins that are accessible through the ImageJ web page (Rasband,1997-2008, Castleman, 2005, Miller, 2002).

References

Abramoff, MD, Magelhaes, PJ, Ram, SJ, Image Processing with ImageJ, Biophotonics International (2004), **11**(7)**:**36-42

Berend N, Salome CM, King GG, Mechanisms of airway hyper-responsiveness in asthma. Respirology (2008), **13**(5):624-631

Burger W and Burge MJ, Digital Image Processing - An Algorithmic Approach using Java. Springer-Verlag, New York (2008). ISBN 978-1-84628-379-6, www.imagingbook.com

Cabrera JE, "GLCM_Texture" plug-in for ImageJ, (2005), http://rsb.info.nih.gov/ij/plugins/

Castleman M, "Cell_outliner" plug-in for ImageJ (m@mlcastle.net), Columbia University (2005) http://rsb.info.nih.gov/ij/plugins/cell-outliner.html

Chicco P, Magnussen JS, Mackey DW, Bush V, Emmett L, Storey G, Bautovich G, and Wall H van der, SPET of a computerised model of diffuse lung disease, Eur.J.Nuc.Med (2001), **28**(2)**:**150-154

Choi HK, New Methods for Image Analysis of Tissue Sections. PhD thesis, Uppsala University, Sweden (1996), ISBN 91-554-3829-6

Clausi DA, An analysis of co-occurrence texture statistics as a function of grey level quantization. Can. J. Remote Sensing, (2002), **28**(1):45–62

Cradduck TD, Bailey DL, Hutton BF, Conninck F De, Busemann-Sokole E, Bergmann H, and Noelpp U, A standard protocol for the exchange of nuclear medicine image files. NucMedComm (1989), **10**:703-713

Downie SR, Salome CM, Verbanck S, Thompson BR, Berend N and King GG, Ventilation heterogeneity is a major determinant of airway hyperresponsiveness in asthma, independent of airway inflammation. Thorax (2007), **62**:684-689

Haralick RM, Shanmugam K, and Dinstein I, Textural features for image classification. IEEE Transactions on Systems, Man, and Cybernetics (1973), SMC-**3**(6):610-621

Haralick RM, Statistical and structural approaches to texture. Proceedings of the IEEE 67 (1979), **5**:786-804

Harris BE, Bailey D, Miles S, Bailey E, Rogers K, Roach P, Thomas P, Hensley M, and King GG, "Objective analysis of tomographic ventilation perfusion scintigraphy in pulmonary embolism", Am. J. Respir. Crit. Care Med. , March 15, 2007

Haynor DR, Harrison RL, Lewellen TK, The use of importance sampling techniques to improve the efficiency of photon tracking in emission tomography simulations. Med Phys (1991), **18**:990–1001

King GG, Eberl S, Salome CM, Meikle SR, and Woolcock AJ, Airway closure measured by a Technegas bolus and SPECT. Am.J.Respir.Crit.CareMed. (1997) **155**:682–688

King GG, Eberl S, Salome CM, Young IH, and Woolcock AJ, Differences in airway closure between normal and asthmatic subjects measured with single-photon emission computed tomography and technegas. Am.J.Respir.Crit.CareMed. (1998), **158**:1900–1906.

Lewellen TK, Anson CP, Haynor DR, Design of a simulation system for emission tomographs. J Nucl Med (1988), **29**:871

Miller M, "Segmenting_Assistant", plug-in for ImageJ, (2002) mmiller3@iupui.edu, http://rsb.info.nih.gov/ij/plugins/index.html

Parker JA, Align3_TP: stack alignment plug-in for ImageJ, J.A.Parker@IEEE.org (version 25/Mar/2008), http://www.med.harvard.edu/JPNM/ij/plugins/Align3TP.html

Petersson J, Sánchez-Crespo A, Larsson SA and Mure M, Physiological imaging of the lung: single-photon-emission computed tomography (SPECT). J Appl Physiol (2007) **102**:468-476

Rasband, W.S., ImageJ, U. S. National Institutes of Health, Bethesda, Maryland, USA, http://rsb.info.nih.gov/ij/, 1997-2008.

Tgavalekos NT, Musch G,Harris RS, Vidal Melo MF, Winkler T, Schroeder T, Callahan R, Lutchen KR and Venegas JG, Relationship between airway narrowing, patchy ventilation and lung mechanics. Eur Respir J (2007), **29**:1174–1181

Venegas JG, Schroeder T, Harris S, Winkler RT, and Vidal Melo MF, The distribution of ventilation during bronchoconstriction is patchy and bimodal: A PET imaging study. Respiratory Physiology & Neurobiology (2005) **148**:57–64

WHO World Health Organisation, 2008a, http://www.who.int/respiratory/asthma/en/

WHO World Health Organisation, 2008b, http://www.who.int/respiratory/copd/en/

Xu J, Moonen M, Johansson Å, Gustafsson A, and Bake B, Quantitative analysis of inhomogeneity in ventilation SPET. Eur J Nucl Med (2001) **28**:1795–1800

Zubal IG, Harrell CR, Smith EO, Rattner Z, Gindi G, Hoffer PB, Computerized three-dimensional segmented human anatomy. Med Phys (1994), **21**:299–302

Appendix A: Definition of textural features from the co-occurrence matrix

A co-occurrence matrix P(i,j|d,θ) (PM for short) contains the probability that the grey level i occurs at a distance d in direction θ from a pixel with grey value j. N is the size of the co-occurrence matrix (N=256 in this study). Integrated sums are calculated from the matrix variance. We further define the vertical ($p_x(i)$), horizontal ($p_y(i)$), minor diagonal ($p_{x-y}(k)$) sums, the vertical (μ_x) and horizontal (μ_y) mean, and the variance of the vertical (V_x) and horizontal (V_y) directions (Choi, 1996). Note that the GLCM mean is distinct from the mean grey value of the original image because it is weighted by the frequency of occurrence *in combination with* a certain neighbour pixel value.

$P_x(i) = \Sigma_{j=0}^{N-1} PM$, $P_y(i) = \Sigma_{i=0}^{N-1} PM$, $P_{x-y}(k) = \Sigma_{i=0, |i-j|=k}^{N-1} \Sigma_{j=0}^{N-1} PM$, $\mu_x = \Sigma_i i P_x(i)$,
$\mu_y = \Sigma_j j P_y(j)$, $V_x = \Sigma_i (i - \mu_x)^2 P_x(i)$, $V_y = \Sigma_j (j - \mu_y)^2 P_y(j)$

TC_1 Angular Second Moment $\Sigma_{i=0}^{N-1} \Sigma_{j=0}^{N-1} PM^2$

TC_2 Difference Moment or GLCM Contrast $\Sigma_{i=0}^{N-1} \Sigma_{j=0}^{N-1} (i-j)^2 PM$

TC_3 Inverse Difference Moment, $\Sigma_{i=0}^{N-1} \Sigma_{j=0}^{N-1} (1 + (i-j)^2)^{-1} PM$

TC_4 Diagonal Moment, $\Sigma_{i=0}^{N-1} \Sigma_{j=0}^{N-1} \overline{0.5(i-j)} PM$

TC_7 Inertia, $\Sigma_{n=0}^{N-1} n^2 \left[\Sigma_{i=0, |i-j|=n}^{N-1} \Sigma_{j=0}^{N-1} (i-j)^2 PM \right]$

TC_9 GLCM Correlation, $\left[\Sigma_{i=0}^{N-1} \Sigma_{j=0}^{N-1} (ij) PM - \mu_x \mu_y \right] / \sqrt{V_x V_y}$

TC13 GLCM Variance, V_x

TC18 Coefficient of Variation, $\sqrt{V_x V_y} / \mu_x \mu_y$

TC21 Entropy, $\Sigma_{i=0}^{N-1} \Sigma_{j=0}^{N-1} (PM) (-\ln (PM))$

TC23 Difference Entropy, $\Sigma_{i=0}^{N-1} P_{x-y}(i) \log_e [P_{x-y}(i)]$

TC30 Local Homogeneity. $\Sigma_{n=0}^{N-1} [P_{x-y}(n) / (1+n^2)]$

TC31 GLCM Mean $0.5(\mu_x + \mu_y)$

histogram	cube side length in [mm]	TC_1 Angular Second Moment	TC_3 Inverse Different Moment	TC_4 Diagonal Moment	TC_9 Correlation	TC18 Coefficient of Variation	TC21 Entropy	TC30 Local Homogeneity	TC13 Sum of squares /Variance	TC31 Mean	TC13/ TC31 Variance /Mean ratio
cs	2.5	111.9	4.2	-27.1	-15.2	22.5	-8.4	4.2	-2.2	-10.6	9.5
cs	5.0	106.4	7.5	-27.3	-20.0	28.9	-8.0	7.5	-16.8	-19.6	3.5
cs	7.5	85.8	9.0	-23.3	-22.3	46.6	-6.7	9.0	-17.7	-25.1	9.8
cs	10.0	68.6	10.5	-20.2	-19.2	77.0	-5.6	10.5	-15.6	-30.9	22.2
cs	**mean**	**93.2**	**7.8**	**-24.5**	**-19.2**	**43.7**	**-7.2**	**7.8**	**-13.1**	**-21.6**	**11.3**
hm	2.5	111.9	2.3	-27.2	-11.7	-0.7	-8.4	2.3	-0.4	0.1	-0.6
hm	5.0	106.4	-0.4	-24.9	-15.6	-0.1	-8.0	-0.4	-0.3	-0.1	-0.2
hm	7.5	85.8	0.4	-21.5	-16.1	-1.0	-6.8	0.4	-1.3	-0.2	-1.1
hm	10.0	68.6	2.1	-18.7	-13.8	0.1	-5.6	2.1	-1.1	-0.6	-0.5
hm	**mean**	**93.2**	**1.1**	**-23.1**	**-14.3**	**-0.4**	**-7.2**	**1.1**	**-0.8**	**-0.2**	**-0.6**

Table 1: Sensitivity of textural parameters to a 40% reduction in ventilated lung volume. The latter was achieved by randomly inserting black cubes of side length 2.5, 5, 7.5 and 10mm into the simulated lung. Results are shown as relative changes in the textural parameter for either preparing the data in a histogram-matched (hm) or a contrast-stretched (cs) way and as a mean over 5 distances used in the GLCM calculation.

Histogram	TC 1 Angular Second Moment	TC 3 Inverse Different Moment	TC 4 Diagonal Moment	TC 9 Correlation	TC18 Coefficient of Variation	TC21 Entropy	TC30 Local Homogeneity	TC13 Sum of squares (Variance)	TC31 Mean	TC13/ TC31 Variance /Mean ratio
cs	-62.6	-2.9	53.4	10.8	-10.8	11.5	-2.9	8.7	10.4	-1.5
hm	-62.3	-3.9	48.5	9.0	0.5	11.3	-3.9	-0.1	-0.3	0.2

Table 2: Sensitivity of textural parameters to a 40% increase in gamma counts. The simulated defects have a cube side length of 10mm. Listed are the differences in the values of the textural parameters derived from either the standard simulation with 40% NVV and associated drop in average brightness and an alternative simulation with a higher gamma count such that after knocking out 40% of the ventilated volume the IOD matched the IOD of the perfectly ventilated lung simulation.

Figure captions

Figure 1: *Illustration of textural parameter TC18, Coefficient of Variation, from the simulation study for cube-shaped defects of size 7.5mm cube side length as a function of non-ventilated lung volume in percent. The GLCMs were created for 5 pixel distances each (1, 2, 4, 8, 12 pixels) corresponding to distances in the lung of 4.7, 9.3, 18.7, 37.3 and 56.0mm, respectively. The coefficient of variation is larger for small pixel distances and increases with NVV and more rapidly so for larger defects (not illustrated).*

Figure 2: *Relative ventilated lung volume (solid black) and standard variation (hashed) per patient group.*

Figure 3: *Illustration of textural parameter TC18, the Coefficient of Variation, for a set of 5 'normal' lungs (left) and a set of 5 lungs of patients suffering from COPD (right). The severity of COPD increases from top to bottom.*

Figure 4: *Textural parameter 18 (solid black) and standard deviation (hashed) from the invariant GLCM and for all 5 distances for the 5 patient groups studied*

Figure 5: *Ratio of textural parameter 30/31 (solid black) and standard deviation (hashed) from the invariant GLCM and mean over 5 distances for the 5 patient groups studied*

Figure 6: *High correlation between ventilated lung volume in percent and textural parameter 18 (coefficient of variation) (r^2=0.955).*

Figure 7: *Correlation between textural parameter TC13/TC31 (Variance over Mean ratio) and independent spirometry data (FeV1) for 4 of the 5 patient groups. No spirometry data was available for the 'normal' group. The quality of the linear regression is r^2=0.66.*

FIGURE 1

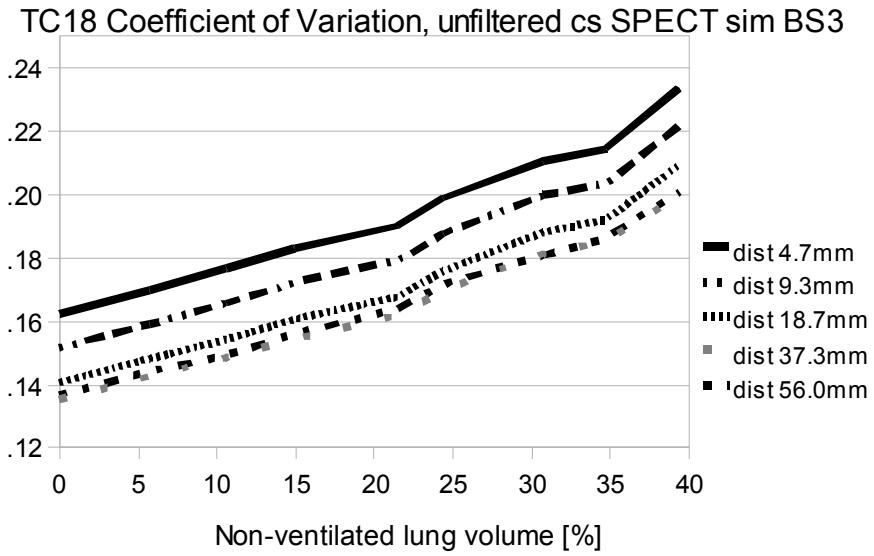

FIGURE 2

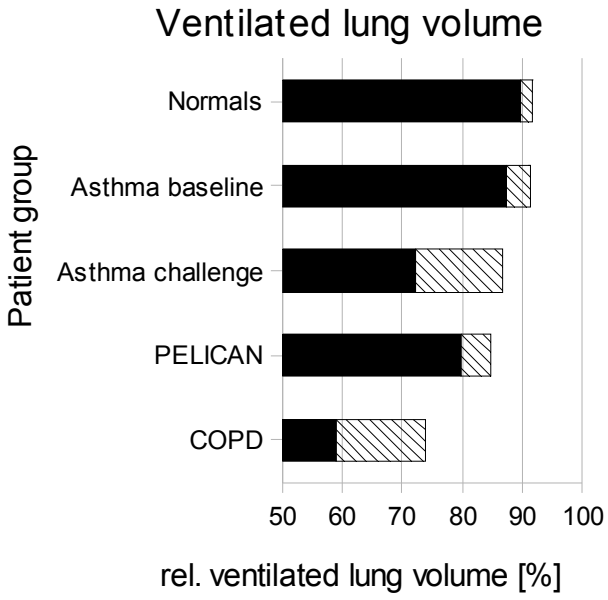

FIGURE 3 (left and right panel, reproduction in black-and-white)

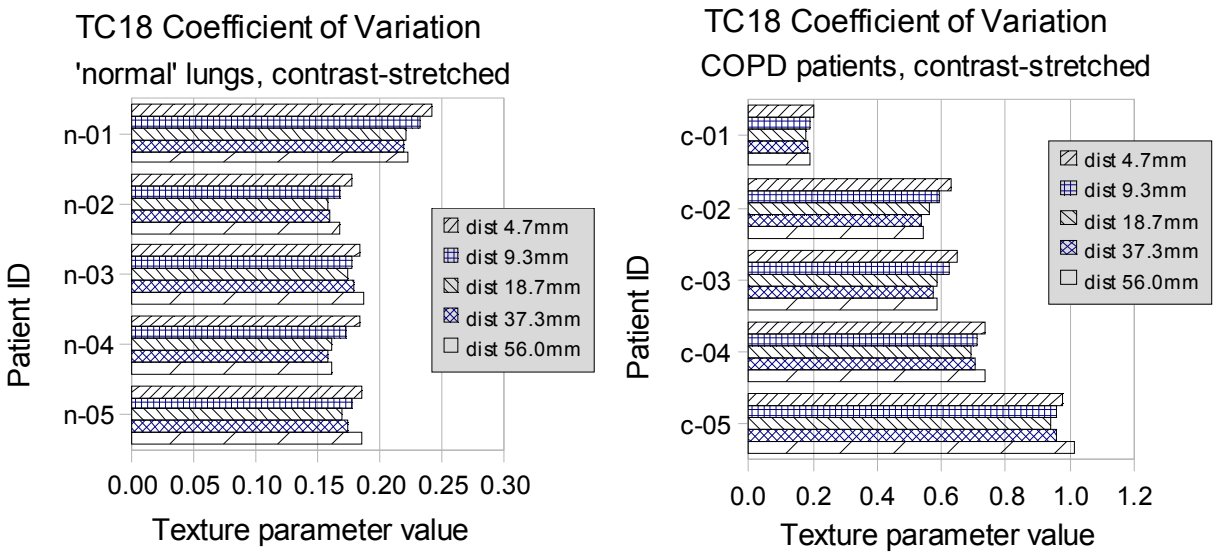

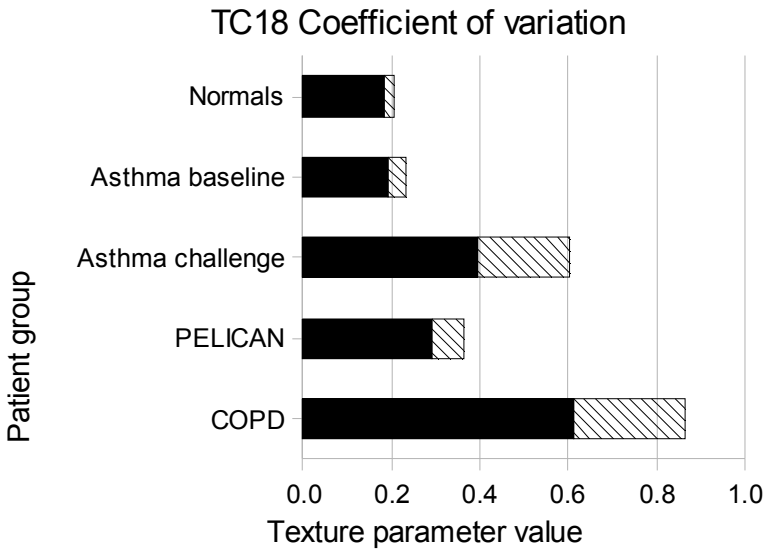

FIGURE 4

FIGURE 5

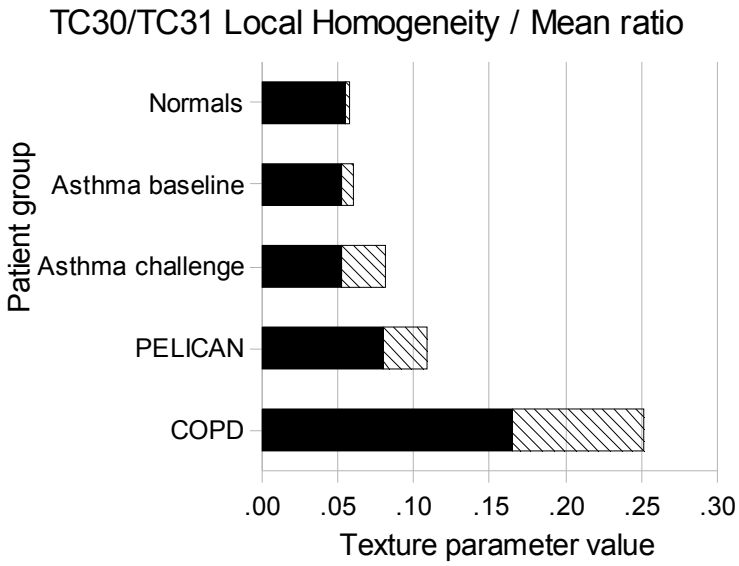

FIGURE 6 (colour reproduction for web-publishing, black-and-white for print)

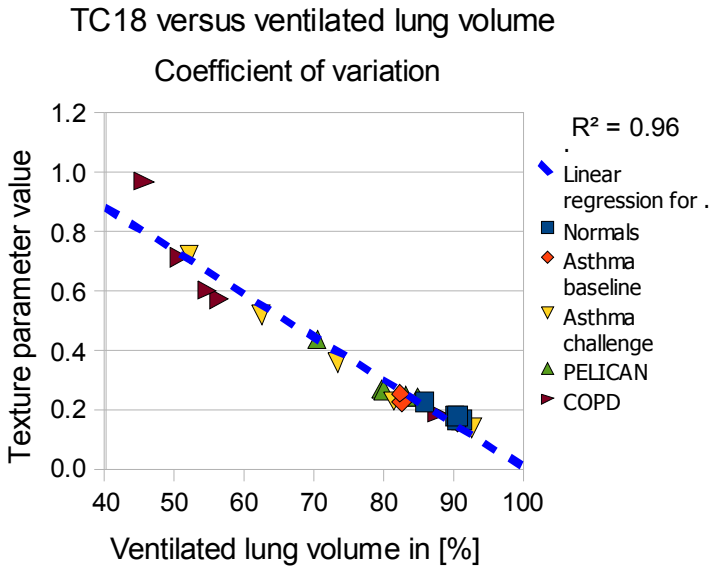

FIGURE 7 (colour reproduction for web-publishing, black-and-white for print)

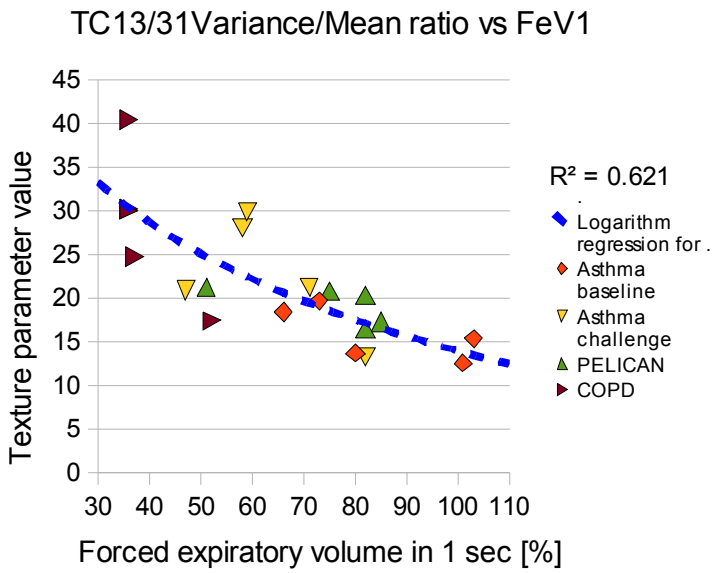

Sydney, 8 December, 2008

Dr Arndt Meier
Electron Microscope Unit
Australian Key Centre for Microscopy and Microanalysis
Madsen Bldg F09, Room 270
Sydney University NSW 2006, AUSTRALIA

phone +61 2 9036 6417
fax +61 2 9351 7682
a.meier@usyd.edu.au
www.emu.usyd.edu.au

To:
The editor
Computerized Medical Imaging and Graphics

Dear editor,

we are submitting the manuscript

Application of Texture Analysis to Functional Pulmonary CT Data

Arndt Meier[a], Catherine Walsh[b,c,d], Benjamin E. Harris[b,c,d], Gregory G.King[b,c,d], and Allan Jones[a]

a) Australian Key Centre for Microscopy and Microanalysis, The University of Sydney, Sydney 2006, NSW, Australia, email: a.meier@usyd.edu.au *(corresponding author)*

b) Department of Respiratory Medicine, Royal North Shore Hospital, St Leonards NSW 2065

c) Woolcock Inst. of Medical Research, 431 Glebe Point Road, Glebe, NSW 2037

d) Northern Clinical School, Faculty of Medicine, University of Sydney, Sydney, 2006

for publication in the journal Computerized Medical Imaging and Graphics. The work is new and genuine and has not been published previously in this or any other form nor has it been submitted to any other publisher. All studies involving human subjects have been conducted in accordance with international and local ethics requirements.

This statement is made on behalf of all authors of the manuscript.

The manuscript was prepared in OpenOffice and then exported to MS Word data format. We are additionally sending a copy in PDF format as a 'ground-truth' in the unlikely event that tables or formulas look corrupted after importing the manuscript into a genuine MS Office application. Please notify us should this happen so we can fix any problems.

We believe that the material presented is of interest to your readers and that it has been prepared in a diligent way and that it meats all criteria for submission. We are happy to clarify any questions you or the reviewers may have.

Kind Regards,

Arndt Meier